FUSE

Fungal Systematics and Evolution

VOLUME 17
JUNE 2026
PAGES 139–156

Bridging the gap between genetic discovery and formal taxonomy: An integrative description of *Nosema slupiense sp. nov*. (*Microsporidia*) from freshwater amphipod *Gammarus pulex*

M. Ovcharenko[1], A. Rashydov[2], K. Bącela-Spychalska[3], J. Manuel Leiro[4], R. A. Sueiro[4], M. Oros[2], V. Sarabeev[2,5]*

[1]Institute of Biology, Pomeranian University of Słupsk, Arciszewskiego 22b, 76200, Słupsk, Poland
[2]Institute of Parasitology, Slovak Academy of Sciences, Hlinkova 3, 04001 Košice, Slovak Republic
[3]Department of Invertebrate Zoology and Hydrobiology, Faculty of Biology and Environmental Protection, University of Lodz, Banacha 12/16, 90-237 Lodz, Poland
[4]Institute for Aquatic Environment and One Health Research (iARCUS), Universidade de Santiago de Compostela, and Health Research Institute of Santiago de Compostela (IDIS), 15782, Santiago de Compostela, Spain.
[5]Department of Biology, Zaporizhzhia National University, Universitetska 66, 69011 Zaporizhzhia, Ukraine

*Corresponding author: volodimir.sarabeev@gmail.com; sarabeev@saske.sk

Keywords:
comparative molecular analysis
diversity
light and ultrastructural data
new taxa
Octo-, tetra- and hexasporous sporogony
taxonomy

Abstract: While recent molecular studies have identified a significant number of putative new species of the genus *Nosema* in amphipod hosts, the vast majority remain formally undescribed. This creates a critical gap between genetic discovery and formal taxonomy, which this study aims to bridge by providing an integrative description of a new microsporidian, *Nosema slupiense sp. nov.*, parasitising the freshwater amphipod *Gammarus pulex*. We combined light and transmission electron microscopy with multilocus molecular analysis of the 18S rRNA and *RPB1* genes to characterise the morphology, ultrastructure, life cycle, and phylogenetic position of the parasite. *Nosema slupiense sp. nov.* develops in direct contact with the host cell cytoplasm and infects mainly muscle tissue, suggesting a horizontal transmission pathway. A key finding is the complex life cycle that includes multiple sporogony. The dominant pathway is octosporoblastic, producing uninucleate octospores, but tetra-, hexa-, and rare disporoblastic (producing diplokaryotic megaspores) sequences also occur. Ultrastructurally, the mature spores have a bipartite polaroplast and 11–13 polar filament coils. Phylogenetic analyses of 18S and *RPB1* markers identify *N. slupiense sp. nov.* as a distinct monophyletic lineage within the clade of amphipod-infecting *Nosema* spp. Unique molecular signatures were identified for both gene markers and are supported by diagnostic morphological and ecological characteristics that together unambiguously diagnose the new species. Infection prevalence showed seasonal variation but no significant female bias, suggesting a lack of feminising capability. By establishing a crucial link between the unique life cycle of *Nosema slupiense sp. nov.*, with its ancestral octosporous development, and its distinct molecular profile, our results extend the known diversity and developmental plasticity within the genus. This integrative work underscores the necessity of combining morphological and genetic data and allows us to propose refined divergence thresholds for the 18S and *RPB1* markers to improve future species delimitation in this complex group.

Citation: Ovcharenko M, Rashydov A, Bącela-Spychalska K, Leiro JM, Sueiro RA, Oros M, Sarabeev V (2026). Bridging the gap between genetic discovery and formal taxonomy: An integrative description of *Nosema slupiense sp. nov.* (*Microsporidia*) from freshwater amphipod Gammarus pulex. *Fungal Systematics and Evolution* **17**: 139–156.
Received: 27 October 2025 ; **Accepted:** 17 April 2026; **Effectively published online:** 20 June 2026
Corresponding editor: P.W. Crous

INTRODUCTION

Although *Microsporidia* have been known since the 19th century for their impact on economically important animals such as silkworms, fish, and crustacea, their taxonomy at higher and species levels remains poorly understood and controversial (Naegeli 1857, Quiles *et al.* 2020, Park & Poulin 2021, Bojko *et al.* 2022, Bacela-Spychalska *et al.* 2023, Stratton *et al.* 2024). *Nosema bombycis* (Naegeli 1857), a silkworm parasite, was the first microsporidian described (Franzen 2008). Since then, more than 1300 species from over 220 genera have been reported (Park & Poulin 2021), exhibiting a diversity of life cycles, host specificity, and transmission routes (Stentiford *et al.* 2013b, Bojko *et al.* 2022), and infecting tissues such as muscle, connective tissue, haemolymph, and gonads (Stentiford & Dunn 2014, Weigand *et al.* 2016, Bacela-Spychalska *et al.* 2018).

Microsporidia are ubiquitous intracellular pathogens of all animal groups (Stentiford *et al.* 2013a, b, Bojko *et al.* 2022), are commonly found in amphipod crustaceans (Bojko & Ovcharenko 2019), and exhibit high morphological plasticity, giving rise to cryptic species that are now being elucidated using molecular phylogenetics (Stentiford *et al.* 2013b, Bojko *et al.* 2015). Amphipods, which play a key role in aquatic food webs (Giari *et al.* 2020, Shaw *et al.* 2020), include *Gammarus pulex,* widely distributed in the middle and lower parts of European streams and rivers with low and moderate water velocities (Karaman & Pinkster 1977).

Recent molecular studies revealed a high diversity of the genera *Cucumispora*, *Nosema*, and *Dictyocoela* in European amphipods (Quiles *et al.* 2019, 2020, 2021), with multispecies infections in *G. pulex* (Grabner *et al.* 2015). Bacela-Spychalska *et al*. (2023) found 39 *Nosema* haplogroups clustered in five clades and predicted new candidate species. Nevertheless, few species of *Nosema* have been formally described from various animal taxa, and only *N. granulosis* is known from amphipods (Terry *et al.* 1999). This parasite is characterised by a monomorphic life cycle, ungrouped spores, and a granular polaroplast. In most cases, the emphasis on large-scale molecular screening has not been accompanied by morphological investigations, thereby limiting the accuracy of species delimitation and description (Nadler & De León 2011, Scholz 2024). Accurate taxonomic assignment and clarification of host specificity remain critical, as many microsporidian taxa display a narrow host range, which underpins their ecological and evolutionary significance (Harrison & Larson 2014, Chethana *et al.* 2021, Park & Poulin 2021, Willis & Reinke 2022).

This study addresses the taxonomic gap by combining light and electron microscopy with multilocus genotyping to clarify the species boundaries of *G. pulex*-infecting microsporidians. During field work in the Baltic region of Poland (2020–2021), the genera of *Dictyocoela*, *Nosema*, and *Mrazekia* were detected (Sarabeev *et al.* 2023a, b, 2024, Sarabeev & Ovcharenko 2024). At one locality, infections with octosporous sporogony and mononuclear spores resembled *Dictyocoela* spp., but matched *N. granulosis* in 18S rRNA. Subsequent intensive sampling and sequencing of material from this locality, using two molecular markers (18S rRNA and *RPB1*), revealed the presence of three distinct clades of *Nosema* species. The accumulated morphological and molecular data currently allow us to molecularly and morphologically characterise and describe a new species, which we introduce here as *Nosema slupiense sp. nov.* The developmental data indicate common features with other *Nosema* species, including diverse spore forms, and suggest a greater diversity than previously recognised.

MATERIAL AND METHODS

Study material and field collection

Amphipod samples were collected from two localities in Pomerania, Poland: a tributary stream of the Słupia River near Krępa Słupska (54°24’12.14”N, 17°2’49.24”E) and the Orzechowa stream, a tributary of the Baltic Sea (54°35’55.83”N, 16°55’7.83”E) (Table 1). Sampling was performed using a standard kick sampling technique by V. Sarabeev and M. Ovcharenko between September 2020 and April 2021, and by M. Ovcharenko in November 2022. Gammarids were brought to the laboratory alive in the boxes for dissection within 48 h. Individuals that were not dissected within 24 h were kept in the refrigerator (at approx. 4–8 °C). Only adult gammarids with a length of 6.2–15.8 mm were analysed. Amphipods were identified using the morphological characters described in the available keys (Karaman & Pinkster 1977, Eggers & Martens 2001) and confirmed with COI barcoding following the procedure described in Królikowska *et al.* (2024). Microsporidian infections were identified morphologically and molecularly as described in Sarabeev *et al.* (2023b) and Sarabeev & Ovcharenko (2024).

Microscopic methods

The collected gammarids were examined under a stereo microscope (SMZ-161 with digital camera Moticam BTU). Each anatomical unit (body surface with muscles, intestine, hindgut, organs of the body cavity and gills) was prepared and examined separately under a compound microscope (Delta Optical Evolution 300). Parasites were identified to the nearest taxonomic level based on the sporogenesis morphology. Subsequently, selected pieces of infected tissues were preserved in 100 % ethanol for molecular analysis. Air-dried tissue smears prepared from adult specimens were fixed with methanol and stained with Giemsa (Becnel 2012). Spores and developmental stages were measured using EPview Image Analysis Software (Olympus Soft Imaging Solutions GmbH). The smears from specimens KSGP9, KSGP14, KSGP41 and KSGP46 were used for description and measurements of hapantotypes (Supplementary file 1).

Ultrastructural studies were carried out by transmission electron microscopy (TEM) as previously described by Leiro *et al.* (1996) and Paramá *et al.* (2006). Amphipod samples were dissected in 2.5 % glutaraldehyde buffered with 0.1 M sodium cacodylate buffer, pH 7.2. After rinsing in cacodylate buffer and post-fixation in 1 % osmium tetroxide, prestained in saturated aqueous uranyl acetate, dehydrated in a graded acetone series to 100 % acetone and embedded in Spurr’s resin. Ultrathin sections were cut with an ultratome (Reich-Jung, UltracutE, Austria) and stained with alcoholic uranyl acetate and lead citrate and viewed in a Jeol JEM-1011 (Japan) electron microscope at an accelerating voltage of 80 kV.

DNA extraction, amplification and sequencing

After visually inspecting amphipod individuals for microsporidian infection, alcohol-preserved host specimens were dried, and total genomic DNA was extracted using a simplified protocol by Keeney *et al*. (2007). This method utilised Chelex 100 (Bio-Rad Laboratories, CA, USA) and Proteinase K, following the specific procedure detailed in Sarabeev *et al*. (2025). The amplification was performed using general microsporidian primers targeting the small subunit ribosomal RNA gene (18S rRNA, SSU) and the large subunit RNA polymerase II (*RPB1*) genes. The forward V1f (5’-CACCAGGTTGATTCTGCCTGAC-3) and reverse 1492r or 1342R (5’-GGTTACCTTGTTACGACTT-3’ or 5’-ACGGGCGGTGTGTACAAAGAACAG-3’) were used to amplify and sequence the SSU rRNA marker (Zhu *et al.* 1993, Stentiford *et al.* 2018). These primer sets generate up to 1150 bp of microsporidian rRNA amplicons. Some of the sequences were also obtained using the reverse primer 530R (5’-CCGCGGCKGCTGGCAC-3’) (Huang *et al.* 2004) paired with V1f. For the *RPB1* gene, two non-overlapping fragments (F2 and F4) were amplified and sequenced as follows to Bacela-Spychalska *et al*. (2023). The F2 fragment was amplified using primers F2f (5’-GKT GTG GRA ATA AAC AGC-3’) and F2r (5’-TCT ACT CTC TTM CCC ATA AG-3’), generating a 520 bp amplicon. The F4 fragment was amplified using primers F4f (5’-GAA AGA CAC ATG CAG RAT

Table 1. Characteristics of examined microsporidian isolates from *Gammarus pulex* collected from a tributary stream of the Słupia River near Krępa Słupska (KS) and Orzechowa stream (OS), Poland, including GenBank accession numbers, voucher material information, and illustrations

Isolate ID	Date	Locality	Parasite species	18S				*RPB1*							Material deposited	Comment
								F2 fragment			F4 fragment			Haplogroup		
				Label on figure	Accession number	Sequence length	Haplogroup	Label on figure	Accession number	Sequence length	Label on figure	Accession number	Sequence length			
KSGP2	30.11.2022	KS	*N. slupiense sp. nov.*	KSGP2 *N. slupiense* sp nov Gpul PL	PX314004	1024	2_14	F2 F4 KS2GP *N. slupiense* sp nov Gpul PL	PX390150	514	F2 F4 KS2GP *N. slupiense* sp nov Gpul PL	PX394764	606	2_43	-	b
KSGP3	30.11.2022	KS	*Nosema* sp.	KSGP3 *Nosema* sp Gpul PL	PX314013	990	3	-		-	- F4 KSGP3 *Nosema* sp Gpul PL	PX394772	612	No enough data	#SLTC072403 Voucher	b
KSGP5	30.11.2022	KS	*Nosema* sp.	KSGP5 *Nosema* sp Gpul PL	PX314014	1042	5	F2 - KSGP5 *N. slupiense* sp nov Gpul PL	PX390156	521	-		-	-	-	-
KSGP9	30.11.2022	KS	*N. slupiense sp. nov.*	KSGP9 *N. slupiense* sp nov Gpul PL	PX314012	1088	9	-		-	-		-	-	#SLTC072408 Hapantotype	a, b, c; Fig. 4 (H, I, W, R, U)
KSGP14	30.11.2022	KS	*N. slupiense sp. nov.*	KSGP14 *N. slupiense* sp nov Gpul PL	PX314007	1038	2_14	F2 F4 KSGP14 *N. slupiense* sp nov Gpul PL	PX390151	505	F2 F4 KSGP14 *N. slupiense* sp nov Gpul PL	PX394767	600	14_20_45	#SLTC072409 Hapantotype	a, b, c; Fig. 4 (B, G, E, F, J, M - Q, X, Z ,AA)
KSGP15	30.11.2022	KS	*Nosema* sp.	-		-	-	F2 F4 KSGP15 *Nosema* sp Gpul PL	PX662004	453	F2 F4 KSGP15 *Nosema* sp Gpul PL	PX662004	522	15	-	b
KSGP20	30.11.2022	KS	*N. slupiense sp. nov.*	KSGP20 *N. slupiense* sp nov Gpul PL	PX314016	1055	20_22_23_41_43_51	F2 F4 KSGP20 *N. slupiense* sp nov Gpul PL	PX390158	504	F2 F4 KSGP20 *N. slupiense* sp nov Gpul PL	PX394774	609	14_20_45	-	b
KSGP23	30.11.2022	KS	*N. slupiense sp. nov.*	KSGP23 *N. slupiense* sp nov Gpul PL	PX314019	1019	20_22_23_41_43_51	F2 F4 KSGP23 *N. slupiense* sp nov Gpul PL	PX390159	509	F2 F4 KSGP22 *N. slupiense* sp nov Gpul PL	PX394776	612	22_23_41_47	#SLTC072404 Paratype	b
KSGP22	30.11.2022	KS	*N. slupiense sp. nov.*	KSGP22 *N. slupiense* sp nov Gpul PL	PX314015	1048	20_22_23_41_43_51	F2 F4 KSGP22 *N. slupiense* sp nov Gpul PL	PX390157	507	F2 F4 KSGP23 *N. slupiense* sp nov Gpul PL	PX394773	612	22_23_41_47	-	b
KSGP29	30.11.2022	KS	*Nosema* sp.	KSGP29 *Nosema* sp Gpul PL	PX314017	1026	29	F2 F4 KSGP29 *Nosema* sp Gpul PL		453	F2 F4 KSGP29 *Nosema* sp Gpul PL	PX394775	543	29	-	-
KSGP32	30.11.2022	KS	*Nosema* sp.	*Nosema* sp Gpul PL	PX314009	1006	32_47_49	-		-	- F4 KSGP32 *Nosema* sp Gpul PL	PX394769	447	No enough data	-	b
			N. slupiense sp. nov.	-		-	-	F2 - KSGP32 *N. slupiense* sp nov Gpul PL	PX390154	498	-		-	No enough data		

KSGP41	30.11.2022	KS	*N. slupiense sp. nov.*	KSGP41 *N. slupiense* sp nov Gpul PL	PX314008	1051	20_22_23_41_43_51	F2 F4 KSGP41 *N. slupiense* sp nov Gpul PL	PX390153	502	F2 F4 KSGP41 *N. slupiense* sp nov Gpul PL	PX394768	600	22_23_41_47	#SLTC072407 Hapantotype	a, b, c; Fig.4 (A, B)
KSGP43	30.11.2022	KS	*N. slupiense sp. nov.*	KSGP43 *N. slupiense* sp nov Gpul PL	PX314010	1046	20_22_23_41_43_51	F2 F4 KSGP43 *N. slupiense* sp nov Gpul PL	PX390155	504	F2 F4 KSGP43 *N. slupiense* sp nov Gpul PL	PX394770	612	2_43	-	b
KSGP45	30.11.2022	KS	*N. slupiense sp. nov.*	-		-	-	F2 F4 KSGP45 *N. slupiense* sp nov Gpul PL	PX662005	451	F2 F4 KSGP45 *N. slupiense* sp nov Gpul PL	PX662005	600	14_20_45	#SLTC072410 Hapantotype	a, b, c; Fig.4 (C, D, K, L)
KSGP46	30.11.2022	KS	*Nosema* sp.	KSGP46 *Nosema* sp Gpul PL	PX314005	1013	-	-		-	- F4 KSGP46 *Nosema* sp Gpul PL	PX394765	546	No enough data	-	b
KSGP47	30.11.2022	KS	*N. slupiense sp. nov.*	-		-	-	F2 F4 KSGP47 *N. slupiense* sp nov Gpul PL		454	F2 F4 KSGP47 *N. slupiense* sp nov Gpul PL	PX394771	600	22_23_41_47	#SLTC072405 Voucher	b
			Nosema sp.	KSGP47 *Nosema* sp Gpul PL	PX314011	1065	32_47_49	-		-	-		-	-		
KSGP49	30.11.2022	KS	*Nosema* sp.	KSGP49 *Nosema* sp Gpul PL	PX314006	1065	32_47_49	-		-	- F4 KSGP49 *Nosema* sp Gpul PL	PX394766	606	No enough data	-	-
KSGP51	30.11.2022	KS	*N. slupiense sp. nov.*	KSGP51 *N. slupiense* sp nov Gpul PL	PX685592	1008	20_22_23_41_43_51	-		-	-		-	-	#SLTC072406 Hapantotype	a, b, c, d; Figs 4-6.
KSGP53	30.11.2022	KS	*Nosema* sp.	-		-	-	F2 - KSGP53 *Nosema* sp Gpul PL	PX390152	504	-		-	-	-	-
GP36O	21.10.2020	OS	*N. slupiense sp. nov.*	GP36O *N. slupiense* sp nov Gpul PL	PX314003	436	No enough data	-		-	-		-	-	#SLTC072411 Voucher	b
KSGP31	30.11.2022	KS	*Dictyocoela duebenum*	KSGP31 Dictyocoela duebenum	PX314018	1098	-	-		-	-		-	-	-	b
GP30O	21.10.2020	OS	*Dictyocoela duebenum*	GP30O Dictyocoela duebenum	PX314002	449	-	-		-	-		-	-	-	b

*a. Measurements of Giemsa-stained smear (Supplementary file 1). b. Stained microscope slide. c. Micrographs, presented in this paper. d. Tissues embedded in Spurr's resin.

G-3') and F4r (5'-TTC CWG ACA TGA TYT CTC C-3'), generating a 640 bp amplicon. The PCR mixtures and reaction conditions for obtaining SSU sequences were carried out as described by Sarabeev et al. (2023b), and those for *RPB1* were performed as outlined by Bacela-Spychalska *et al*. (2023). The PCR products were verified by electrophoresis on a 1 % agarose gel in sodium tetraborate buffer containing GelRed nucleic acid stain (Merck) to confirm the presence of bands of the expected size under variable intensity at 300 nm using the Gel Doc EZ Gel Documentation System (BioRad, USA). The PCR products were then purified with ExoSAP-IT™ and sequenced in both directions using the Sanger sequencing service (SEQme, Czech Republic).

Sequence processing and alignment procedures

Forward and reverse contigs were assembled using Geneious Prime (Geneious development team 2025) and compared to GenBank entries with BLAST (Boratyn *et al.* 2013). The sequences of 18S rRNA and *RPB1*, including the F2 and F4 fragments, were trimmed to final size ranges of 436–1098 bp, 451–521 bp, and 522–612 bp, respectively, as detailed in Table 1. Trimming was performed according to sequence quality and utilising a de novo assembly algorithm with predetermined removal of low-quality regions in Geneious Prime. The sequences obtained in the present study have been deposited in GenBank (Table 1). The translation of *RPB1* sequences into amino acids was carried out using the standard translation table to check for the presence of stop codons. The phylogenetic analysis was focused on sequences of *Nosema* species, including all haplogroups identified by Bacela-Spychalska *et al*. (2023), available in GenBank as of June 2025. By haplogroups, we mean the same as defined by Quiles et al. (2019) and Bacela-Spychalska *et al.* (2023); that is, sequences of each marker were assigned to haplogroups by clustering two sequences into a single haplogroup based on 100 % pairwise nucleotide identity in their shared region, with each haplogroup defined by diagnostic SNPs. All sequence fragments were aligned separately. For the 18S rRNA marker, alignment was performed using Clustal Omega v. 1.2.2 (Sievers *et al.* 2011). Both fragments of the *RPB1* marker were aligned using the Translation Align algorithm with the legacy gap penalty option, as implemented in Geneious Prime. Obtained alignments were visually checked for quality and realigned if needed. F2 and F4 fragments were concatenated in Geneious Prime after filling the missing sequence ends with "N".

Detection of diagnostic molecular characters

The sequence alignments that served as the basis for the selection of diagnostic nucleotides are presented in Figs 1 and S1 for the 18S and *RPB1* markers, respectively. These alignments included only unique 57 *Nosema* sequences for the 18S rDNA and 86 and three sequences of *Nosema* spp. and *Vairimorpha* spp. for the *RPB1* marker. All duplicates were removed before analysis. For the *RPB1* marker, only samples containing both F2 and F4 sequence fragments were included. Primer sets are indicated on the consensus sequences within each alignment. Diagnostic nucleotides are reported by their positions in the consensus sequence of each alignment, with position 1 defined as the first nucleotide of the forward primers: V1f and F2f. To identify diagnostic molecular characters for species delimitation, the aligned sequences for single-nucleotide polymorphisms (SNPs) using the variant detection tool in Geneious Prime with default options were analysed.

The sequence variation was further examined using the Characteristic Attribute Organisation System (CAOS) approach as described in (Bergmann & Hadrys 2009) to detect and categorise discrete, species-specific nucleotide characters. CAOS distinguishes single-nucleotide and multinucleotide attributes, i.e "single character attributes" and "compound character attributes", classifying them as pure (present in all members of a clade and absent from others) or private (present in some, but not all, members of a clade and absent from other clades). Given the relatively low informativeness of the 18S marker, manually identified pure compound character attributes, mapped after SNPs were aligned, were used to characterise new species. For the more variable *RPB1* marker, SNP-based single-character attributes were used for diagnostic purposes.

Phylogeny reconstruction of the genus *Nosema*

The generated 18S and *RPB1* databases were subsequently processed to trim primer ends and remove short sequences. During manual curation, we aimed to retain all possible haplogroups and preserve maximal phylogenetic information. Following this procedure, sequences were checked for duplicates, which were then removed. The sequence obtained in the present study was supplied with the number of duplicates reduced. The final alignments used in the phylogenetic analysis are presented in Table S1 (partial 18S rDNA gene, 992 bp) and Table S2 (partial *RPB1* gene, 871 bp, F2 and F4 fragments), both comprising 42 sequences (http://purl.org/phylo/treebase/phylows/study/TB2:S32248?x-access-code=6a8641381c371ec08fe04c4dc62dcc88&format=html). *Vairimorpha* spp. were chosen as an outgroup for *RPB1* dataset, as representatives of the closely related genera (Tokarev *et al.* 2020), while the most distant congeneric species, *Nosema pilicornis*, was used to root the 18S tree.

Phylogenetic reconstructions were performed separately for 18S rRNA and *RPB1* sequences using Bayesian inference as implemented in MrBayes v. 3.2.7a (Ronquist & Huelsenbeck 2003). JModelTest v. 2.1.10 was employed to select the best-fitting model of nucleotide substitution (Darriba *et al.* 2012). For both SSU and *RPB1*, we used the Hasegawa-Kishino-Yano (HKY) model, selected as the best fit for each gene based on model testing. The HKY model incorporated invariant sites for the 18S dataset and Gamma-distributed rate variation for the *RPB1* dataset, reflecting the optimal configuration as indicated by model testing. All codon positions were used for phylogenetic analyses. Markov chain Monte Carlo analysis was run for one million generations, with the first 250 sampled trees (representing the initial 25 % of generations) discarded as burn-in. Posterior probabilities were estimated from the remaining trees, and a half-compatible consensus tree was generated. The trees were visualised using FigTree v. 1.4.4 (http://tree.bio.ed.ac.uk/software/figtree/).

Genetic dissimilarity among *Nosema* species was calculated from the trimmed, aligned sequences as both the

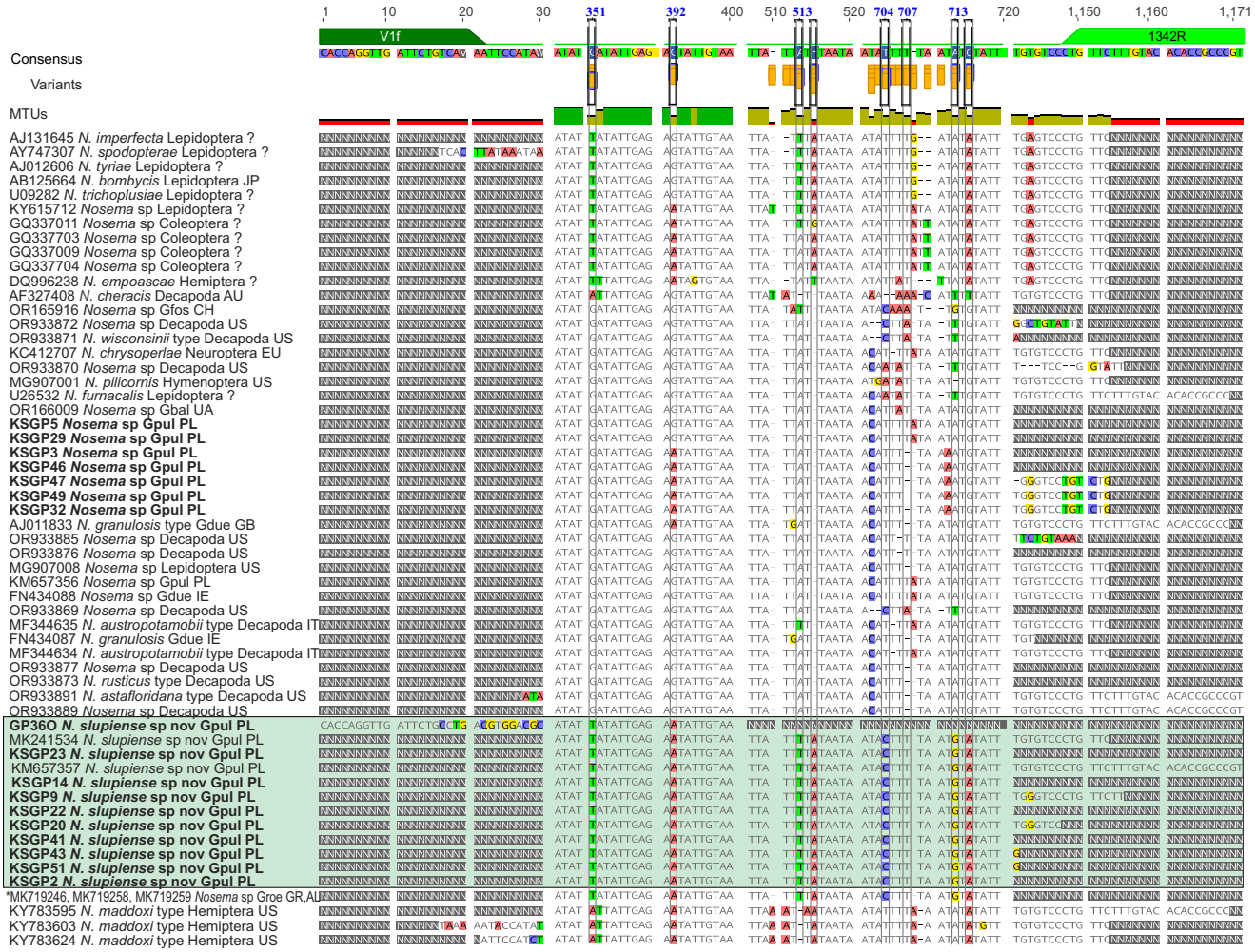

Fig. 1. Overview of the amino acid alignment of the 18S rRNA marker for *Nosema* species with single-nucleotide sequence variations (SNPs) analysis. Sequences obtained in the present study are shown in bold. Used primer set (V1f and 1342R) and SNPs annotated on the consensus sequence. Single nucleotide polymorphisms with adjusted synonymous characters from the alignment, useful for identifying new species, were shown to emphasise informative positions, thereby facilitating the identification of sequence differences among taxa. Shaded N indicates the absence of nucleotides. The sequence labels include the GenBank accession number or, for sequences generated in this study, the isolate number, parasite species name, host species order, and the country's ISO code. If parasite sequences are obtained from amphipods, the labels provide information on the abbreviated host species name (Gbal – *Gammarus balcanicus*, Gdue – *Gammarus duebeni*, Gfos – *Gammarus fossarum*, Gpul – *Gammarus pulex*, Groe – *Gammarus roeselii*). The data obtained in this study are highlighted in bold, with the number of host individuals for each haplogroup shown in brackets (if applicable). Samples marked with * represent a short 18S fragment (716 bp) from *G. roeselii* collected in Greece and Albania; these sequences are identical to *Nosema slupiense sp. nov.*, but multilocus *RPB1* data place them in a closely related yet distinct lineage (Figs 3, S1).

percentage and the absolute number of pairwise nucleotide differences, with gaps excluded. The results were visualised as heatmaps in Figs S2 and S3.

We used the Assemble Species by Automatic Partitioning (ASAP) method to delineate molecular operational taxonomic units (MOTUs) potentially representing species within the *Nosema* clade (Puillandre *et al.* 2021). ASAP analysis was performed locally using the desktop GUI (ASAPy v. 1.0) from iTaxoTools (https://itaxotools.org). For this analysis, we specified the simple distance (p-distance) as the evolutionary model. ASAP takes as input a set of aligned sequences, calculates pairwise genetic distances, estimates a distance threshold, and then proposes species partitions, which are ranked using a scoring system that does not incorporate any prior biological information about intraspecific diversity. The genetic distance matrix for ASAP was generated for the *RPB1* sequence database and not for 18S rDNA. The 18S gene is highly conserved and exhibits low sequence variability (Hadziavdic *et al.* 2014, Bacela-Spychalska *et al.* 2023, Stratton *et al.* 2024), especially for closely related taxa, resulting in a weak contrast between intra- and interspecific genetic distances. Additionally, our 18S dataset was mainly composed of taxa represented by a single individual, whereas reliable species delimitation with ASAP requires multiple individuals per species (Puillandre *et al.* 2021). This combination of limited variability and low sampling is insufficient for the robust detection of a distinct barcode gap, which is fundamental for pairwise distance-based species delimitation methodologies such as ASAP. The use of such conserved markers may lead to artificial lumping or the failure to resolve species boundaries (Carstens *et al.* 2013, Puillandre *et al.* 2021).

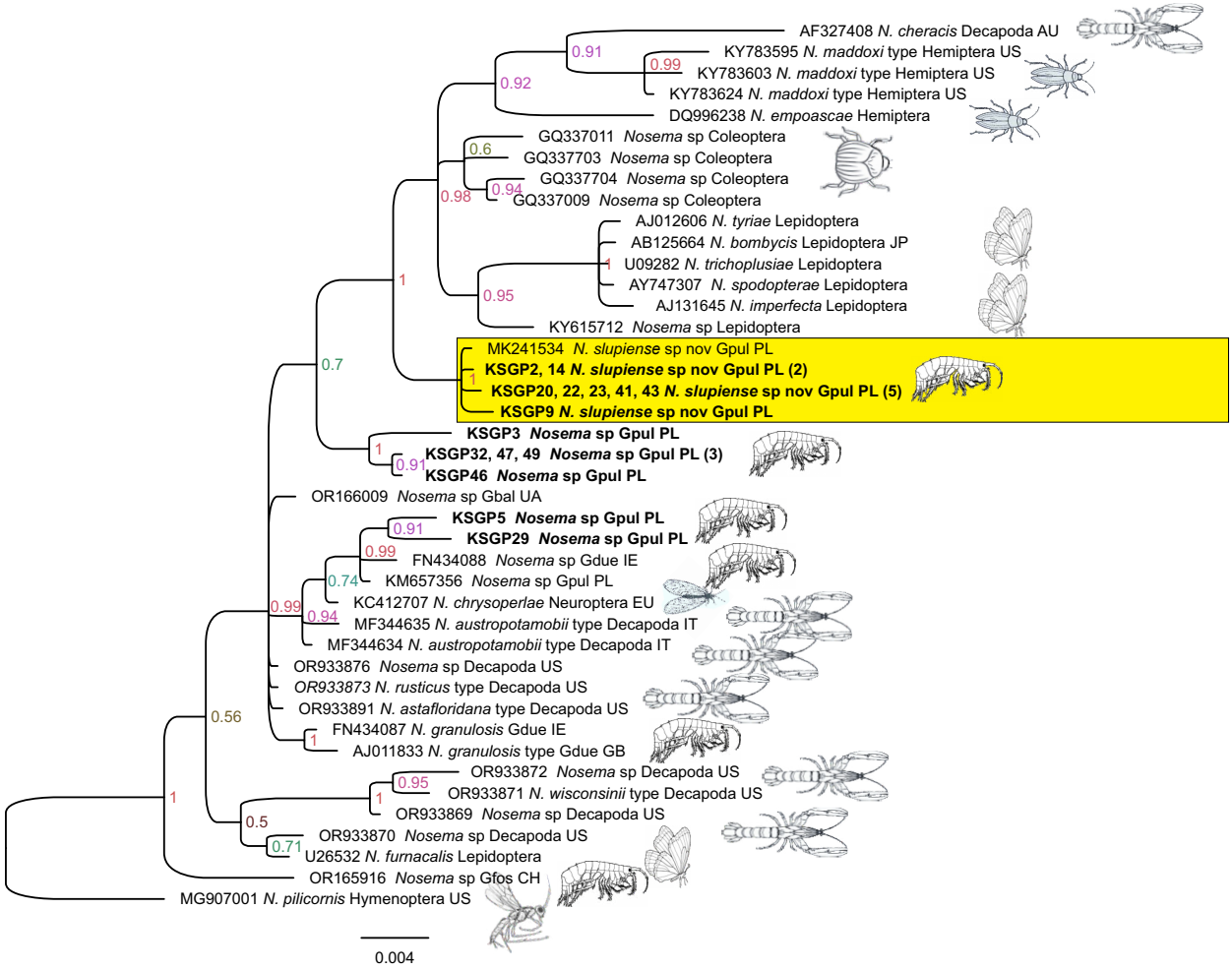

Fig. 2. Bayesian phylogenetic reconstruction for 42 sequences of *Nosema* spp. based on 992 bp of the 18S marker, rooted to *Nosema pilicornis*. A shaded rectangle highlights the new species. The analysis utilised the Hasegawa-Kishino-Yano (HKY) model, which incorporates invariant sites, making it the best fit for the sequence data. The sequence labels are as in Fig. 1. Sequence alignments for all species included in the analysis are provided in Supplementary Table S1.

RESULTS

Infection rates and diagnostic insights

Of the 92 adult specimens of *G. pulex* collected from the stream near Krępa Słupska in spring 2021, 12 individuals (13 %, Wilson score confidence interval (CI): 7.6–21.4 %) were infected with microsporidians. In contrast, the prevalence of infection was much higher in autumn, 20 out of 56 individuals (16 males and 4 females out of 35 males and 21 females examined) were positive at this site (35.7 %, CI: 24.5–48.8 %). The sample from autumn 2022 was subjected to full sequencing, which allowed the prevalence of the new species to be accurately determined. Molecular analyses of this sample revealed that 11 (nine males and two females) of 56 individuals (19.6 %, CI: 11.3–31.8 %) harboured the new species, including two cases of co-infection with *Nosema* sp. Furthermore, 10 individuals (17.9 %, CI: 10.0–29.8 %) were infected with *Nosema* sp., including cases of co-infection with the new species, while one individual (1.8 %, CI: 1.0–3.0 %) was infected with *Dictyocoela duebenum* (Table 1). In the autumn sample of *G. pulex* from the Orzechowa stream, octospores were detected in six of 34 examined individuals (17.7 %, CI: 8.3–33.5 %). This infection represents a combination of *Dictyocoela* spp. and *Nosema* spp. (Table 1). In all cases, the infection was systemic and characterised by a particularly heavy infestation of the muscle tissue, with both vegetative stages and mature spores present. The infection was mainly observed in the muscles of both female and male hosts. Heavily infected specimens often showed a white mass under the cuticle and in the muscles. The presence of numerous tetra- or octospores enclosed in sporophorous vesicles was registered.

Phylogenetics

Genetic variation and haplogroups of new species: The partial 18S rDNA sequences of the analysed *Nosema* isolates were highly conserved, and none of the 91 SNP variants identified for this marker could unambiguously characterise the *N. slupiense sp. nov.* (Fig. 1). SNP analysis of the variable RPB1 marker revealed over one thousand variants across the F2 and F4 fragments, with the F4 fragment being much more variable and containing four unique single-character

positions specific to the new species (Fig. S1). The final alignment, with trimmed ends and reduced duplicate sequences, revealed the presence of three haplogroups of *Nosema slupiense sp. nov.* for both gene markers in our samples (Figs 2, 3, S2 and S3) (Table 1). For the 18S marker, an additional haplogroup was identified, represented by the sequence #MK241534 from the same host, *Gammarus pulex*, sampled in the Warsaw district, Poland, and available in GenBank. Isolates KSGP22, KSGP23, and KSGP41 were consistently assigned to the same haplogroup according to both the 18S and RPB1 markers. The incongruence between the gene markers observed for the haplogroup formed by isolates KSGP2 and KSGP14, as indicated by the 18S marker, could indicate co-infection of the host with different individuals of the same species. The differences between the haplogroups of *Nosema slupiense sp. nov.* were 1–3 bp (0.1–0.3%) for the 18S marker and 1–2 bp (0.1–0.2%) for the *RPB1* marker (Figs S2 and S3). The most divergent 18S rRNA sequence originated from GenBank and was sampled from a different locality in central Poland, in contrast to our samples from Pomerania.
Phylogenetic relationships: The phylogenetic analyses based on both 18S rRNA and *RPB1* gene markers consistently show several strongly supported clades within the genus *Nosema*, reflecting both host associations and evolutionary relationships. Analysis of both phylogenetic trees reveals consistent clustering between markers, revealing congruent groupings for the major lineages. *Nosema slupiense sp. nov.* is robustly nested within the *Nosema* clade with high support from 18S and *RPB1* markers (Figs 2, 3), and all corresponding haplogroups are assigned to the same clade in each analysis. These haplogroups form a well-supported, monophyletic lineage exclusively associated with *G. pulex* from Poland. The 18S gene tree resolves these haplogroups within a strongly supported lineage (posterior probability = 1.00), while the *RPB1* gene tree recovers the clade with moderate support (posterior probability = 0.83), indicating clear genetic distinctness of the new species.

Within the broader *Nosema* phylogeny, *Nosema* species identified from decapod hosts (*N. astafloridana*, *N. austropotamobii*, *N. rusticus*, *N. wisconsinii*, except for *N. cheracis*) form a basal group relative to the clade containing *N. slupiense sp. nov.* and *Nosema* sp. from amphipods, as evidenced by both gene trees (Figs 2, 3). The SSU tree identified three main groups within the genus *Nosema*: a crown clade comprising isolates closely related to terrestrial lepidopteran, hemipteran, and coleopteran hosts; a basal clade containing a diverse assemblage of hosts from both terrestrial and aquatic environments; and a central group primarily restricted to aquatic amphipods (Fig. 2). A similar clustering is observed in the *RPB1* tree, although this marker lacks sequences for the majority of terrestrial hemipteran and coleopteran hosts (Fig. 3). This indicates that the new species has a divergent evolutionary history, aligning more closely with *Nosema* clades infecting amphipod hosts, rather than those found in decapods and terrestrial arthropods. However, host switching with subsequent speciation also appears to be a common evolutionary event in *Nosema*. This pattern is well demonstrated by *N. cheracis*, which, although a decapod parasite from Australia, is genetically associated with both the predominant decapod and amphipod-associated groups.
Genetic dissimilarity: All sequences of *Nosema slupiense sp. nov.* form a genetically cohesive group, with minimal intraspecific dissimilarity, and differ well from all other known *Nosema* taxa (Figs S2 and S3). ASAP reliably differentiated the sequences of the new species, even at a minimal genetic distance of 1 % (Fig. 3). The interspecific dissimilarity was more pronounced for the *RPB1* marker than for 18S (over 13 % and 1.1 %, respectively). Both markers indicate that *N. slupiense sp. nov.* is genetically most similar to *Nosema* species associated with amphipods and decapods, yet clearly and distinctly different from these and all other *Nosema* lineages. The genetic divergence between *N. slupiense sp. nov.* and species infecting terrestrial arthropods (i.e., *Lepidoptera*, *Hemiptera, Hymenoptera*, and *Coleoptera*) is even greater, with pairwise dissimilarities frequently exceeding 2 % for the 18S marker and 20 % for the *RPB1*. Both matrices show pronounced clustering by host group (decapods, amphipods, insects). Within-host group similarity is generally much higher than between-host groups. Concordance between SSU and *RPB1* matrices underscores the robustness of these evolutionary patterns.

Nosema slupiense Ovcharenko, Rashydov, Bącela-Spychalska, Leiro, Sueiro, Oros & Sarabeev, ***sp. nov.*** MB 860842.

Etymology: The species is named for the type locality (a tributary stream of the Słupia River, Pomerania, Poland) in which it was found.

Kingdom: *Fungi* (Wijayawardene *et al.* 2020)
Phylum: *Rozellomycota* (Tedersoo *et al.* 2018, Wijayawardene *et al.* 2020)
Class: *Microsporidea* (Wijayawardene *et al.* 2020)
Order: *Nosematida* (Bojko *et al.* 2022)
Family: *Nosematidae* (Tokarev *et al.* 2020)
Genus: *Nosema* (Tokarev *et al.* 2020)

Typus: **Poland**, Pomeranian Region, tributary stream of the Słupia River near the village Krępa Słupska (54°24’12.14”N, 17°2’49.24”E), from skeletal muscle and haemolymph of *Gammarus pulex* (Amphipoda, Gammaridae), 30 Nov. 2022, *M. Ovcharenko*. Histological slides (#6-8) of hapantotype (KSGP51) are stored at the Research Infrastructures Area, Electron Microscopy, Confocal and Biological Specialties Support Unit, CACTUS Building, University of Santiago de Compostela, Lugo Campus, Spain. Giemsa-stained slides of hapantotypes and paratypes are stored at the Herbarium Slupensis SLTC, deposit-Museum, Institute of Biology, Pomeranian University in Słupsk, Arciszewskiego 22b, 76-200, Słupsk, Poland. The genetic data are deposited in GenBank. The detailed information on accession numbers of the type material and deposited sequences are provided in Table 1.

Additional material examined: **Poland**, Pomeranian Region, Orzechowa stream, tributary of the Baltic Sea (54°35’55.83”N, 16°55’7.83”E), from skeletal muscle of *Gammarus pulex*, 21 Oct. 2020, *V. Sarabeev* & *M. Ovcharenko* (see Table 1).

Note on host genetics: Sequenced host isolates from the type locality infected with *Nosema slupiense sp. nov.* and *Nosema* sp. (KSGP15, KSGP20, KSGP29, KSGP45, KSGP46, KSGP47, KSGP53) were 100 % identical to GenBank sequence

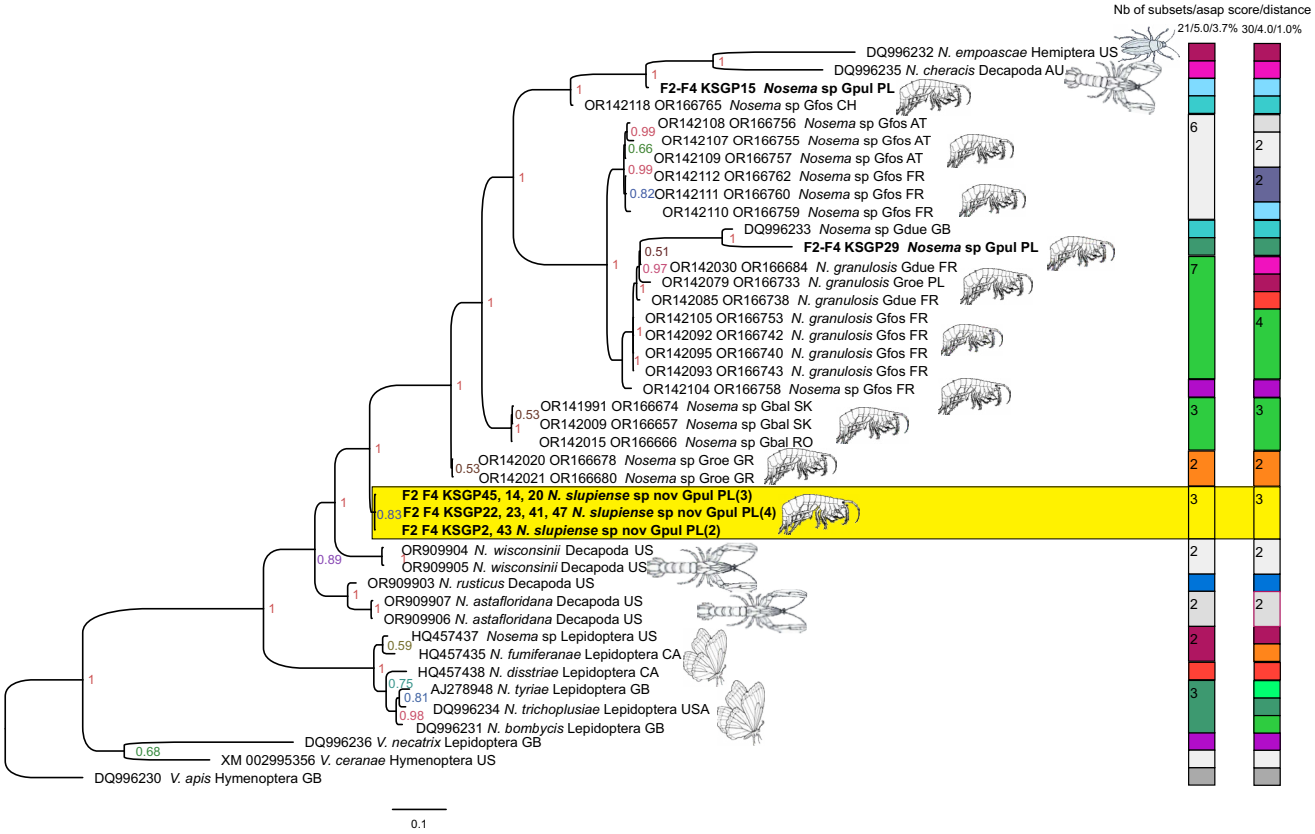

Fig. 3. Bayesian phylogenetic reconstruction for 42 sequences of *Nosema* spp. based on 871 bp of F2 and F4 fragments of the *RPB1* gene with *Vairimorpha* species as the outgroup. The sequence labels are as in Fig. 1. The analysis utilised the HKY model, which incorporates Gamma-distributed rate variation among sites, making it the best match for the given sequence data. The data obtained in the present study are in bold, with the number of host individuals for each haplogroup shown in brackets (if the case). The shaded rectangle highlights the new species. Bars annotated on the right indicate the results of molecular species delimitation obtained using the ASAP method, with the two best partitioning solutions shown based on ASAP scores. Sequence alignments for all species included in the analysis are provided in Supplementary Table S2.

PV705297, corresponding to the widespread in the Baltic Sea drainage system BIN BOLD:ACH6832 (doi.org/10.5883/BOLD:ACH6832). Isolate KSGP23 differed by a single base pair within the 613 bp COI-5P fragment of the host mitochondrial genome (Fig. S4) but was also identified as the same BIN.

Diagnosis of *Nosema slupiense sp. nov.*

Morphology and ultrastructure (Figs 4–6): Merogony occurs in direct contact with the host cell cytoplasm. Uninucleate or binucleate proliferative cells with detached nuclei are generated through plasmotomy of the primary merogonial plasmodium. Each meront of this generation gives rise to a plasmodium containing 4–8 nuclei, which subsequently divides into individual proliferative cells with nuclei organised into diplokaryons. Proliferation of diplokaryotic meronts in a substantial proportion of cells is followed by karyogamy of the diplokaryotic nuclei and meiosis, resulting in the transition from the diplokaryotic stage to the development of octospores or tetraspores. The main sporulation sequence is octosporoblastic and unikaryotic (unikaryotic presporulation developmental stages occur), although tetra- and hexasporoblastic (unikaryotic) and disporoblastic (diplokaryotic) sporogony may also occur. Mature octospores are unikaryotic and ovoid, possessing 11–13 coils of the polar filament. The bipartite polaroplast comprises lamellar and vesicular components. Three spore types, including ovoid octo- and tetrapores and elongate ovoid megaspores. Methanol-fixed and Giemsa-stained octospores measure 2.85±0.29 µm in length and 1.73±0.20 µm in width. Fixed and stained tetraspores measure 3.37±0.22 µm in length and 2.24±0.05 µm in width. Diplokaryotic megaspores measure 3.76±0.32 µm in length and 2.68±0.22 µm in width. The specific parasite of the amphipod *G. pulex* infects skeletal muscle tissue. Description and measurements of hapantotypes in the Supplementary file 1. The diagnostic features that distinguish *Nosema slupiense sp. nov.* from other *Microsporidia* parasitising *G. pulex* are detailed in Table S4.

Molecular characteristics (Figs 1, S1): According to the 18S marker, *Nosema slupiense sp. nov.* differs from all other described *Nosema* species by a unique combination of characters: #704 (state C) and #707 (state T), which corresponds to the multinucleotide variant CTTT, as well as #713 (state G) and #715 (state A), corresponding to the multinucleotide variant GTA (Fig. 1). These two represent a compound pure attribute in terms of CAOS. The *RPB1* marker further supports the uniqueness of *N. slupiense sp. nov.*, as

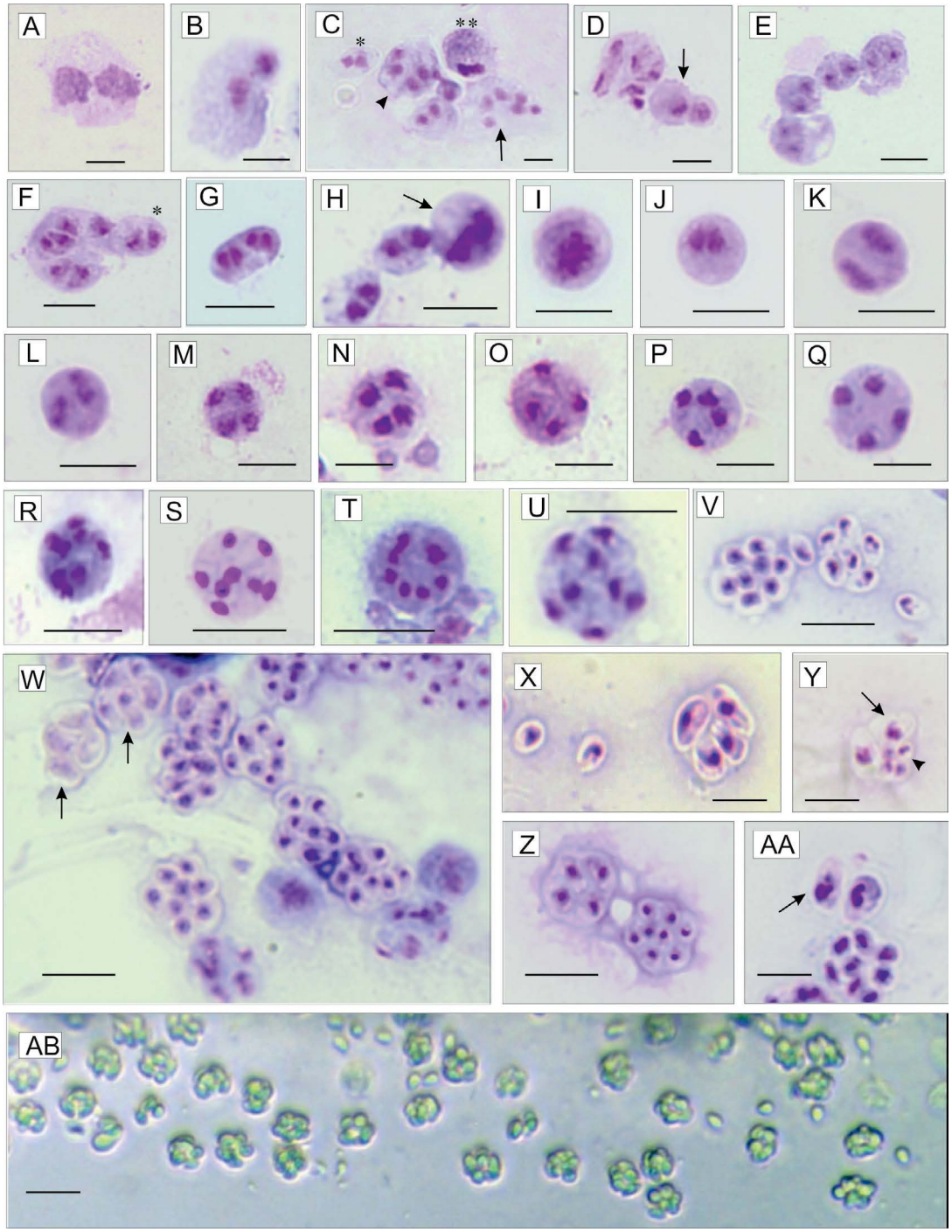

Fig. 4. Light microscope data on the development of *Nosema slupiense sp. nov.* Giemsa-stained slides and fresh spores (AB), Preparation from KSGP9 (H, I, W, R, U); KSGP14 (B, G, E, F, J, M - Q, X, Z, AA); KSGP41(AB); KSGP45 (C, D, K, L); KSGP51 (A, T, V, Y) smears. **A–H.** Proliferative phase. **A.** Early proliferative cell with two big dissociated nuclei. **B.** Proliferative cell with two small nuclei and vacuolized cytoplasm. **C.** Early merogonial plasmodia. Multinucleate (arrow), and fragmentated (arrowhead) plasmodia with separated nuclei, binucleate meront (asterisk), and meront/sporont transitional stage (double asterisk) are visible. **D.** Two uninucleate proliferative cells (arrow) initiate the chain-like formation. **E.** Chain from four binucleate (haploid) meronts with detached nuclei. **F.** Separation of elongate diplokaryotic meront (asterisk) from octonucleate merogonial plasmodium. **G.** Elongate merogonial stage with diplokaryotic nuclei before plasmotomy. **H.** Two diplocaryotic merontes, formed by binary fission of the merogonal stages of the last generation. H (arrowed), **I.** Mononuclear cells with a large nucleus, a product of karyogamy, representing meront/sporont transitional stage. **J–AA.** Sporogonic phase. **J.** Diplokaryotic early sporontal cell. **K.** Binucleate sporont with dissociated nuclei. **L.** The second division of the sporont nuclei results in the formation of a four-nucleate sporogonial plasmodium (**M**). **N, O.** Metamorphosis of tetranucleate sporogonial plasmodium to produce four sporoblasts (tetrasporoblastic sporogony). **P–V.** Octosporoblastic sporogony. The condensed nuclei decrease in size (**P**) and diverge to the periphery of the sporont cell (**Q**). Octonucleate sporogonial plasmodium formed by binary division of each nucleus (**R, S**). Finally, eight sporoblasts are produced after plasmotomy of sporogonial plasmodium (**T, U**). **V.** Mature octospores and two single spores released from damaged sporophorous vesicle (SpoV). **W.** Different stages of sporogenesis. SpoVs containing four spores are arrowed. **X.** Two single octospores and SpoV with tetraspores. **Y.** SpoV enclosing hexaspore formation (featuring two tetraspore size classes and four octospore size classes). Sporogony is probably disrupted due to asynchronous division of the nuclei of the sporogonial plasmodium. **Z.** SpoVs with four and eight spores. **AA.** Two mature diplokaryotic megaspores (arrows) neighbouring SpoV with octospores. **AB.** Nomarski contrast image showing live octospores and isolated spores, released from damaged SpoVs. Bars: 2 µm (A, B); 3 µm (C); 5 µm (D, Q); 4.2 µm (X); 5.5 µm (R, S, V, W,Y, Z, AA); 6 µm (H–U), 6.5 µm (P) ; 7 µm (G); 8.2 µm (AB).

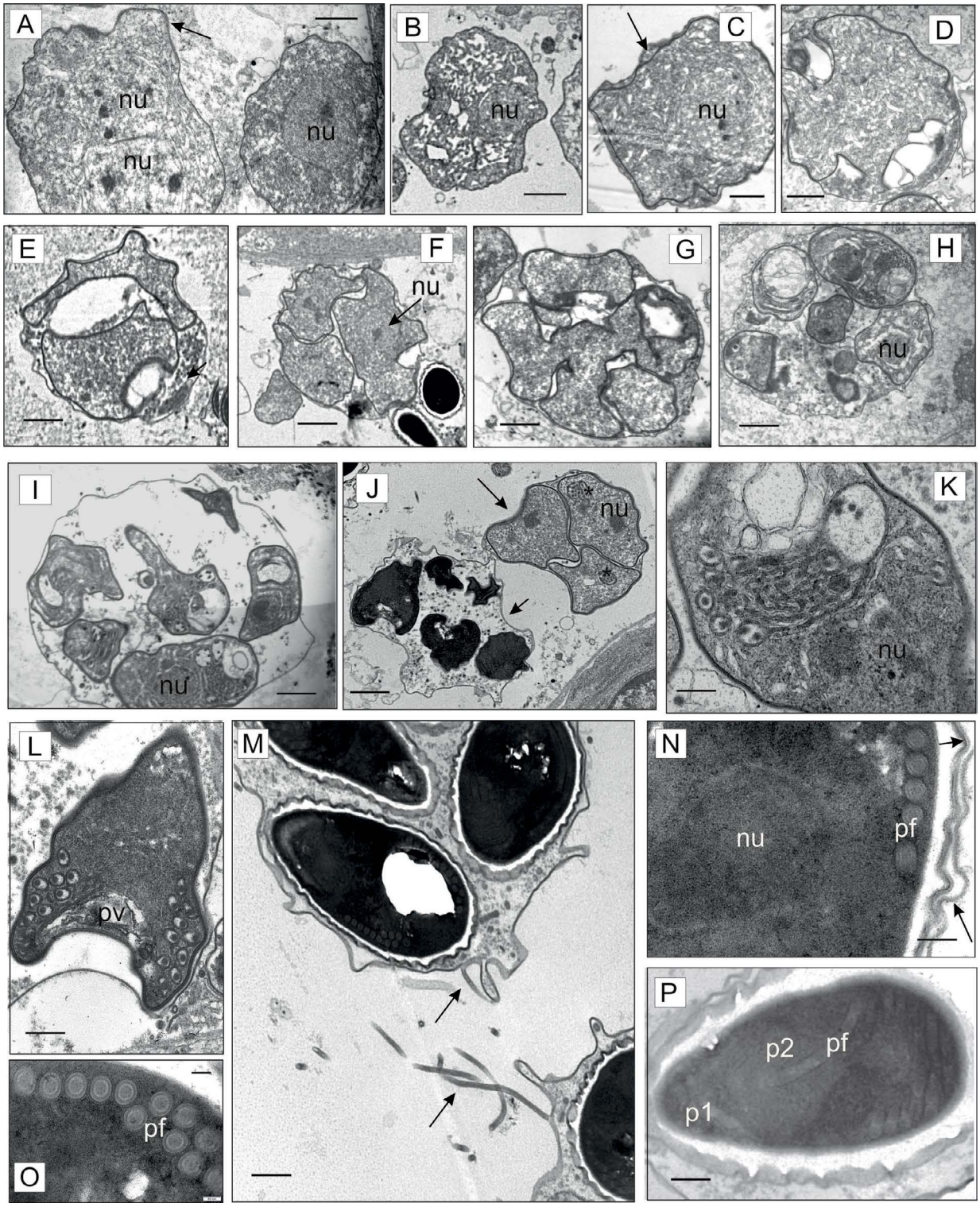

Fig. 5. TEM micrographs illustrating various stages in the development of *Nosema slupiense sp. nov.* **A.** Late meront and meront/sporont transitional cells with paired and separated nuclei (nu). Thickening of the plasma membrane, characterised by a granular accumulation on the late meront surface, indicates the transition to sporogony. **B.** Uninucleate meront/sporont transitional cell with a nucleus (nu), vacuolized cytoplasm, and a thickened cell border. **C.** Increase of sporophorous vesicle (SpoV). A delicate envelope (arrow) covers an early sporont. **D.** Start of plasmotomy of sporogonial plasmodium. **E, F.** Parts of tetrasporous SpoV containing uninucleate sporoblasts and granular material, which developed to form episporontal inclusions (arrowhead). **G.** SpoV with unequal fragmentary sporogonial plasmodium. **H.** SpoV, containing uninucleate sporoblasts of different maturity. Start of sporogenesis. **I.** Octosporous SpoV with late sporoblasts. **J.** Fragments of octosporoblastic SpoV with electron-dense maturated sporoblasts (arrowhead), and tetrasporoblastic SpoV (arrow). Numerous inclusions fill the episporontal space. **K.** Development of polar filament complex in the posterior part of the cell. Vesicular and lamellar structures associated with the formation of polar filament coils are visible. **L.** Posterior part of immature octospore with polar filament coils and posterior vacuole (pv). **M.** Parts of two SpoVs with filamentous protrusions (arrows). **N.** The middle part of a longitudinal section of a mature octospore. Single nucleus (nu), polar filament coils (pf), exospore (arrowhead), and SpoV's wall (arrow) are marked. Exospore consists of an electron-dense basal layer covered by a double-layered membrane. **O.** Ultrastructure of the coiled part of the polar filament (pf). The polar filament consists of several concentric layers of varying thickness and electron density enveloped by the unit membrane. **P.** Oblique cut of the anterior part of a mature octospore. Lamellate (p1) and tubulate (p2) parts of the polaroplast and polar filament (pf) are marked. Bars: 60 nm (O); 120 nm (L, M); 200 nm (P); 250 nm (K); 450 nm (N); 1.0 µm (A); 1.3 µm (I, G, H, C–F); 1.5 nm (B, J).

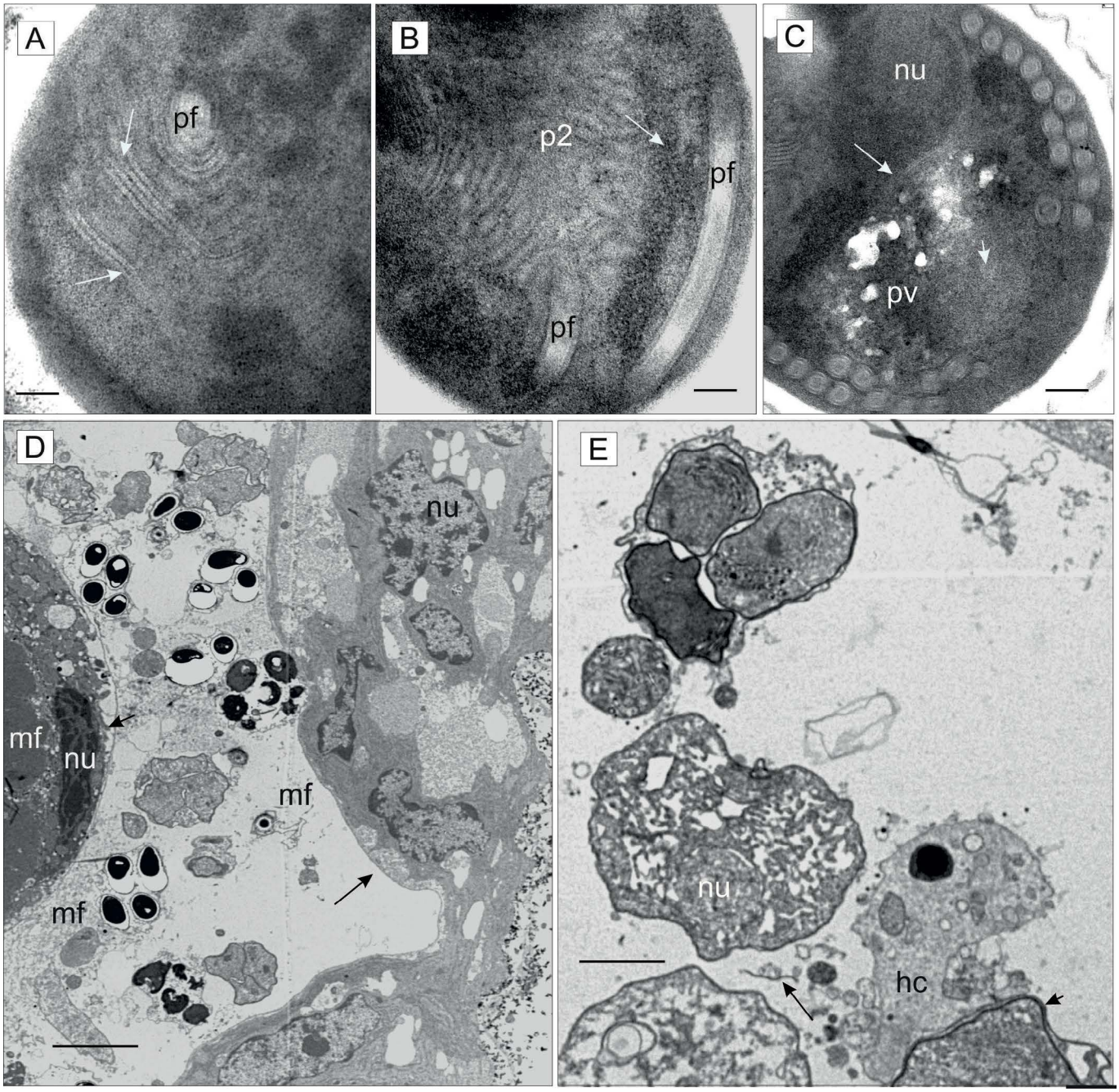

Fig. 6. TEM micrographs of extrusion apparatus structure (**A–C**) of *Nosema slupiense sp. nov.* and haemolymph pathological change (**D, E**). **A.** Transversal section of the anterior region of the polaroplast showing thin lamellae (arrows) surrounding the manubrial part of the polar filament (pf). **B.** Posterior region of polaroplast (p2) with wide lamellate (tubulate) structure. After leaving the polaroplast, the straight part of the polar filament forms a spiral turn. The cytoplasm of a mature spore containing numerous ribosomes is arrowed. **C.** Lateral section of the posterior part of a mature spore showing the nucleus (nu), polar filament coils, and membrane-bound posterior vacuole (pv) containing posterosome (arrowheads). **D.** Spores and sporogony stages located in haemolymphs between adipocytes (arrow) and muscle cells (arrowhead) with a separated nucleus (nu). Haemolymph contains numerous destroyed myofibrils (mf). **E.** Sporophorous vesicles (arrowhead) adhering to a haemocyte (hc) are visible. Bars: 100 nm (A, B); 120 nm (C); 2.0 µm (E); 5 µm (D).

evidenced by pure single character attributes: specifically, character #863 (state A), character #884 (state A), character #905 (state A), and character #1166 (state C) (Fig. S1). These unambiguous synapomorphies uniquely characterise and diagnose *Nosema slupiense sp. nov. Microsporidia* within this species should have 99–100 % similarity to the sequences from type material by the 18S marker and 94.5-100 % similarity by the *RPB1* locus.

DISCUSSION

General context and contribution

As highlighted in the Introduction section, species of four major microsporidian genera, *Nosema* (Bacela-Spychalska *et al.* 2023), *Cucumispora* (Ovcharenko *et al.* 2010, Bojko *et al.* 2015), *Pleistophora* (Terry *et al.* 2003), and *Dictyocoela* (Bacela-Spychalska *et al.* 2018), have been recorded infecting European amphipods. Records of microsporidians

of the genera *Gurleya, Mrazekia, Octospora* require further detailed investigation (Bojko & Ovcharenko 2019). Molecular and morphological studies, particularly in Europe, have revealed an unexpected range of lineages within the genera *Cucumispora*, *Nosema*, and *Dictyocoela*, often within single host populations (Grabner *et al.* 2015, Quiles *et al.* 2019, 2020, 2021, Bacela-Spychalska *et al.* 2023). We contribute to this growing diversity by formally describing a new species, *Nosema slupiense sp. nov.*, and revealing several additional haplogroups representing two new potential species. In addition to the taxonomic benefit, our integrative approach, combining multilocus genotyping, ultrastructural analyses, and comprehensive morphological characterisation, not only bridges the gap between molecular evidence and formal taxonomy but also provides essential baseline data for future epidemiological and ecological studies. Our results improve the understanding of host–parasite specificity, life cycle, and evolutionary relationships of *Microsporidia* in amphipod hosts. This work underscores the necessity of uniting molecular and morphological criteria to refine species boundaries and ensure a robust, reliable taxonomy of parasites, as recommended by Nadler and De León (2011) and Scholz (2024).

Unique biological and life cycle characteristics

The described species is unique among its congeners in that, although rarely, it can undergo not only the typical octosporoblastic (unikaryotic) and disporoblastic (diplokaryotic) sporogony found in most species of *Nosema* (e.g. Tokarev et al. 2020), but also tetra- and hexasporoblastic (unikaryotic) sporogony, producing three types of spores: diplokaryotic megaspores, and unikaryotic tetra- and octospores. Moreover, the most distinctive features of the new species lie in the details of merogony and sporogony, which are unusual for "true" *Nosema* species, especially the amphipod parasite, *N. granulosis*. There are uninucleate or binucleate proliferative cells with separated nuclei (Fig. 4A–D, 5A), rounded merogonial plasmodia (Fig. 4C), meronts that develop into four-cell plasmodia with chain- (binucleate) or ball-shaped (diplokaryotic) configurations (Fig. 4E, F), and diplokaryotic proliferative cells that divide by binary fission (Fig. 4G, H). Proliferation of diplokaryotic meronts in some cells is followed by karyogamy of diplokarya counterparts and meiosis (Fig. 4H, I), thereby switching the diplokaryotic sequence to unicariotic megaspore development. The new species also shows the retention of both sexual and possibly asexual reproductive pathways, in contrast to asexual ones in *N. granulosis*. *Nosema slupiense sp. nov.* has so far been identified infecting only *G. pulex*, suggesting possible strict host specificity. In this study, more than 86 *Nosema* sequences based on the *RPB1* marker and over 55 sequences based on the 18S rDNA were compared (Figs 1, S1). Two sequences from GenBank, retrieved also from *G. pulex* host sampled from the Pomeranian region in Poland, showed 99.7–99.9 % identity with the new species by the 18S marker (Figs 1, S2), clearly representing *Nosema slupiense sp. nov.* Unlike to transovarial transmission of *N. granulosis,* the new species is most likely transmitted horizontally. This is confirmed by its high abundance in muscle tissue. A heavy infestation and the detection of both vegetative and spore stages suggest high pathogenic potential, which may impair host fitness, depress demographic performance (survival and fecundity), and degrade ecosystem functioning (e.g., diminished leaf-litter decomposition, altered food-web dynamics, and shifts in community composition). Among the nosematids, parasitising the muscles of amphipods, high pathogenicity and horizontal transmission have been confirmed in *Microsporidia* of the genus *Cucumispora* (Ovcharenko *et al.* 2010, Bojko *et al.* 2015). Molecular, morphological, ultrastructural and life-cycle data indicate that the microsporidium studied here must be assigned to a species different from all nosematid microsporidians previously described in gammarid hosts. The presence of coinfections, both within individual hosts and between different microsporidian taxa, underscores the need to consider microsporidians as important components of the amphipod microbiome that may influence host health, competition, and community interactions.

The haploid spore sequence in *Nosema slupiense sp. nov.* follows the classical pathway for *Microsporidia* as described by Flegel & Pasharawipas (1995) and confirmed in other studies (Sokolova & Fuxa 2008, Sokolova & Overstreet 2018). In most cases, the two haploid nuclei of an oval diplokaryotic meront (Fig. 4H) fuse to form a single diploid nucleus (Fig. 4I), which then undergoes two standard meiotic divisions to form bi- (Fig. 4J, K) and tetranucleate (Fig. 4M) sporogonial plasmodia, followed by a mitotic division, resulting in the formation of eight haploid nuclei (Fig. 4R, T). However, the final mitotic division in the tetranucleate sporogonial plasmodium is rarely completed for all nuclei or is skipped entirely. This aberrant development leads to the formation of tetrasporous (four-spore) (Fig. 4X) or hexasporous (six-spore) (Fig. 4Y) sporoblasts. The reasons for their formation and their function remain unknown.

Phylogenetic placement and evolutionary context

Phylogenetic analyses based on both 18S and *RPB1* markers clearly assign *N. slupiense sp. nov.* to the amphipod-associated clade within the genus *Nosema,* forming a distinct and monophyletic lineage (Figs 2, 3). The pronounced genetic cohesion within *N. slupiense sp. nov.*, and the clear separation from other congeners, are consistent with patterns expected for distinct *Nosema* species exhibiting host specialisation (Chen *et al.* 2013, Stratton *et al.* 2024, Xiong *et al.* 2024). Importantly, higher interspecific divergence observed for the *RPB1* marker compared to 18S underscores the value of protein-coding loci for microsporidian systematics, particularly when ribosomal markers lack sufficient resolution (Bacela-Spychalska *et al.* 2023, Stratton *et al.* 2024, Bojko *et al.* 2025). Nevertheless, our analyses also revealed that the 18S fragment harboured two hypervariable regions, in nucleotide positions 510–515 and 702–715, that correspond to the V3–V4 region as defined by Hadziavdic *et al.* (2014). This hypervariable segment shows potential for molecular screening and parasite metabarcoding, supporting efficient, high-throughput detection and diagnosis of infection caused by *Nosema* spp., but yields only an approximate estimate of species richness. With respect to *Nosema*, the V3–V4 region appears to provide more information than the V1–V2 and V5 regions, used in previous studies for screening *Microsporidia* (Grabner *et al.* 2015, Quiles *et al.* 2019, 2020, 2021, Trzebny *et al.* 2020, Bacela-Spychalska *et al.* 2023).

Our phylogenetic reconstruction, based on both SSU

and *RPB1* markers, supports three major groups within the genus *Nosema*, comprising both terrestrial and aquatic hosts, with one particular clade mainly associated with aquatic amphipods. This clustering pattern, which is largely consistent across different genetic markers, refines previous understanding (Stratton *et al*. 2024, Bojko *et al*. 2025) by highlighting the complex diversity of host associations within the genus *Nosema.* Nevertheless, phylogenetic proximity observed in several clades, as seen on both the 18S and *RPB1* trees, including *Nosema cheracis* from a decapod host and *Nosema empoascae* infecting a hemipteran host, suggests that host switching between aquatic and terrestrial invertebrates has occurred during the evolutionary history of these parasites. Some of the newly identified haplotypes from this study are closely related to lineages from different ecological backgrounds, providing further evidence of transitions between ecosystems. Our results corroborate recent genomic studies that have identified potential host shift events between bees and wasps in *Nosema*, demonstrating that transitions between distantly related hosts can act as potent drivers of diversification (Xiong *et al.* 2024). Although such host switches are rare, they may have significant implications for our understanding of microsporidian diversification and adaptation.

Implications for taxonomy and species delimitation

From an evolutionary point of view, the genetic analyses support the existence of several haplogroups within *N. slupiense sp. nov.*, with limited but distinct variation for both the 18S and *RPB1* markers. Such genetic structure may arise from microevolutionary processes within host populations, potentially facilitated by host movements and local adaptations. The incongruencies observed between gene markers in certain isolates suggest the possibility of coinfections with different genetic lineages, a phenomenon already described in microsporidians infecting amphipods (Bacela-Spychalska *et al.* 2023). This highlights the importance of both multilocus genotyping as well as next-generation sequencing technologies, which enable the identification of multiple taxa, disentangle complicated infection histories, and the accurate determination of species boundaries.

The classical taxonomy of *Microsporidia* infesting amphipods is largely based on the collection of morphological and ultrastructural data on merogonial and sporogonial developmental features (Sprague *et al.* 1992, Canning & Vávra 2000). According to this approach, the *Microsporidia* parasitising in gammarids can be divided into polysporic (genera *Dictyocoela, Gurleya, Pleistophora*) and disporic (genera *Nosema, Cucumispora*) clades. More recently, the taxonomy of the nosematid microsporidians has undergone extensive revision based on phylogenetic analyses of partial 18S rRNA and *RPB1* gene sequences (Tokarev *et al.* 2020), and has been further corroborated by comprehensive studies utilising a 508-gene concatenated protein phylogeny and a 277-gene concatenated nucleotide phylogeny (Bojko *et al.* 2025). The molecular approach revealed the presence of two distinct clades within nosematid microsporidians: one comprising species closely related to *Vairimorpha necatrix*, the type species of the genus *Vairimorpha*, and the other including species related to *Nosema bombycis*, the type species of the genus *Nosema*. Molecular reclassification of the species revealed that both genera include species with different life cycles, such as those exhibiting diplokaryotic and uninucleate stages, as well as variations in developmental forms previously considered diagnostic for each genus. Recent phylogenetic analyses demonstrated that morphological and ultrastructural criteria, including the presence or absence of octosporogony, are homoplastic and do not reliably reflect evolutionary relationships (Tokarev *et al.* 2020). The octospores are ancestral sexual meiospores that have been lost multiple times within the *Nosema/ Vairimorpha* group (Ironside 2007, Krebes *et al.* 2014). Despite these losses, there is no evidence that any ancient asexual lineages have persisted. The loss of sex has occurred repeatedly but independently rather than resulting in long-term asexual descendants (Ironside 2007, Krebes *et al.* 2014). The described species is an example of the ancestors of the *Nosema/Vairimorpha* group, in which the sexual octospores are unikaryotic, reflecting a classical meiotic pathway in microsporidans (Sokolova & Fuxa 2008, Sokolova & Overstreet 2018). While hexa- and tetrasporoblastic (also unikaryotic) and disporoblastic (diplokaryotic) forms are observed, octosporogony remains the primary route for reproduction of *Nosema slupiense sp. nov.*, producing eight unikaryotic spores each with a single nucleus. The occurrence of diplokaryotic spore types (with two associated nuclei), such as in disporogony, suggests the retention of both sexual and possibly asexual reproductive pathways. This variability of nuclear configuration among spore types highlights the evolutionary plasticity of sexual processes in this group, with unikaryotic stages likely representing the ancestral sexual state and diplokaryotic forms arising as derived or alternative strategies in response to environmental or host-specific pressures.

Our results confirm the findings of Bacela-Spychalska *et al.* (2023), who found a high abundance of *Nosema* spp., with at least five potential species from European gammarid hosts and suggested that this association is ancient. The ASAP partitioning scheme applied to our data further suggests that the current list of *Nosema* species from European amphipods may account for 10–15 species (Fig. 3). This more than two-fold increase in the number of potential species is explained by the fact that our study has added one new species and has also molecularly identified two additional potential species. On the other hand, molecular boundaries for both markers, 18S and *RPB1*, have not yet been established for species delineation within this genus, which could result in varying interpretations of the same data. The 18S marker is a highly conserved gene and, in the case of closely related *Nosema* species, often does not provide sufficient resolution for species-level diagnostics (Pieniazek *et al.* 1996, Tosun 2020, Bacela-Spychalska *et al.* 2023, Stratton *et al.* 2024). For example, this is evident among *Nosema* spp. from lepidopteran hosts and in the recent descriptions of *N. rusticus* and *N. astafloridana* from crayfish (Stratton *et al.* 2024) (Fig. S2). However, 18S marker can still be informative for delineating distinct clades and even species, as demonstrated in this study for *N. slupiense sp. nov.* Although Stratton et al. (2024) stated that microsporidians within *N. wisconsinii*, *N. rusticus*, and *N. astafloridana* should exhibit 98–100 % similarity to the defined type sequence for SSU and *RPB1* loci. However, these thresholds may not be accurate due to the differing variability among genetic markers. For

instance, when this criterion is applied to the 18S marker, a 98–100 % similarity covers the full spectrum of intraspecific variability for haplogroups represented by several species (e.g. MTUs from 22 to 42 according to Fig. S2). Based on the 18S marker dataset used, the interspecific variability shows a similarity of 99.2 % to 99.9 % between haplogroups (e.g. *N. austropotamobii*, *N. granulosis*, *N. maddoxi* and *N. slupiense sp. nov.*). We can conclude that interspecific variability in species delimitation can range from 0.1 % to 0.8 % among haplogroups of a single species, particularly those representing geographically distant populations. In the case of a highly variable *RPB1* marker, a 2 % dissimilarity between groups may hinder a comprehensive delineation of species boundaries. The ASAP partitioning method applied to the *RPB1* database proposed two optimal species assembly variants: one with 30 species at a distance threshold of 1 % and another with 21 species at a threshold of 3.7 %. While the first variant achieved an enhanced ASAP score (Fig. 3), the second variant with 21 species provided a better fit to the clade structure inferred from the MrBayes analysis. Therefore, the threshold of 3.7 % may be more suitable to accurately delineate species boundaries, allowing for a more robust assessment of the clade structure.

Ecological dynamics and absence of feminisation

The prevalence and patterns of microsporidian infection in *G. pulex* observed in this study reveal a complex epidemiological landscape, with overall infection rates varying by season and location. Here, the data show a clear seasonal variation in infection rates, with prevalence peaking in autumn at 35.7 %. The sample from autumn 2022, on which the molecular diagnostics focused, revealed that nearly 20 % of *G. pulex* individuals were infected with the new *Nosema* species. However, an important observation across all samples is that both males and females were similarly affected, and the systemic nature of infection was evident in both sexes. In classical feminising systems, *Microsporidia* exhibit a marked tendency to infect females, an indicator of successful feminisation of genetic males and/or efficient maternal (vertical) transmission, as consistently documented for *Nosema granulosis* and *Dictyocoela* spp. in *Gammarus duebeni* and *G. roeselii* (Kelly *et al.* 2002, Haine *et al.* 2004). The absence of a strong female bias in our samples suggests the new species has limited or no feminising potential under the studied conditions. This conclusion is supported by a recent analysis of diversity of *Nosema* spp. in European gammarids (Bacela-Spychalska *et al.* 2023), which demonstrated that infection patterns consistent with feminisation are restricted to specific clades, notably *N. granulosis* sensu stricto.

CONCLUSIONS

This study provides an integrated morphological, ultrastructural, and molecular characterization of *Nosema slupiense sp. nov.*, a potentially host-specific microsporidian infecting *Gammarus pulex* (BIN: ACH6832) in Poland. This species exhibits octosporoblastic and, occasionally, di-, tetra- and hexasporoblastic sporogony, producing three spore types and retaining both sexual and possibly asexual reproductive pathways, in contrast to *N. granulosis*. It is horizontally transmitted, with high tissue loads in muscle and a high pathogenic potential, which may affect host condition and population dynamics.

Phylogenetic analyses based on 18S rRNA and *RPB1* confirm that *N. slupiense sp. nov.* forms a well-defined monophyletic lineage within the *Nosema* clade associated with amphipods and show that *RPB1* provides greater resolution than 18S for species delimitation. Two additional haplogroups were also identified that may represent new species. The data reinforce the need to combine morphological and molecular criteria, proposing divergence thresholds (3.7 % for *RPB1*) that optimise species delimitation within the group.

Ecologically, infection prevalence varies seasonally, peaking at 35.7 % in autumn, with no significant female bias, suggesting an absence of feminising potential. These findings expand current knowledge on the diversity, evolution, and impact of microsporidians in amphipods and provide a robust basis for future taxonomic, epidemiological, and ecological studies.

ACKNOWLEDGEMENTS

We thank Jaroslaw Brodecki from the Department of Invertebrate Zoology & Hydrobiology, Faculty of Biology and Environmental Protection, University of Lodz, for help in host molecular identification.

FUNDING INFORMATION

A.R. was funded by the EU NextGenerationEU through the Recovery and Resilience Plan for Slovakia under the project No. 09I03-03-V01-00144. This study was partially supported by the Grant Agency of the Ministry of Education of the Slovak Republic and the Slovak Academy of Sciences (project No. VEGA 2/0130/24); Funding to Competitive Reference Groups under reference number ED431C 2025/08 (Xunta de Galicia, Spain), and the Pomeranian University in Słupsk, Poland (project No 7- 4- 9 (64) - B.S. 25.4.9) V.S. is funded by the Seal of Excellence program of the Slovak Academy of Sciences (Project No. SoE/2025/61/MSCA4Uk), and by the International Visegrád Scholarship (No. 52510298). The host molecular identification was financed within PolBOL (https://www.polbol.uni.lodz.pl/) funds.

Conflict of Interest: The authors declare that there is no conflict of interest.

REFERENCES

Bacela-Spychalska K, Wróblewski P, Mamos T, *et al.* (2018). Europe-wide reassessment of *Dictyocoela* (Microsporidia) infecting native and invasive amphipods (*Crustacea*): molecular versus ultrastructural traits. *Scientific Reports* **8**: 8945. https://doi.org/10.1038/s41598-018-26879-3

Bacela-Spychalska K, Wattier R, Teixeira M, *et al.* (2023). Widespread infection, diversification and old host associations of *Nosema* microsporidia in European freshwater gammarids (Amphipoda). (Ed. AR Dillman) *PLOS Pathogens* **19**: e1011560. https://doi.org/10.1371/journal.ppat.1011560

Becnel JJ (2012). Complementary techniques: preparations of entomopathogens and diseased specimens for more detailed study using microscopy. In 'Man. Tech. Invertebr. Pathol.' pp. 451–470. (Elsevier)

Bergmann T, Hadrys H (2009). Character-based DNA barcoding: a superior tool for species classification. *Berliner und Münchener Tierärztliche Wochenschrift* **122**: 446–450. https://doi.org/10.2376/0005-9366-122-446

Bojko J, Dunn AM, Stebbing PD, *et al.* (2015). *Cucumispora ornata* n. sp. (*Fungi: Microsporidia*) infecting invasive 'demon shrimp' (*Dikerogammarus haemobaphes*) in the United Kingdom. *Journal of Invertebrate Pathology* **128**: 22–30. https://doi.org/10.1016/j.jip.2015.04.005

Bojko J, Reinke AW, Stentiford GD, *et al.* (2022). Microsporidia: a new taxonomic, evolutionary, and ecological synthesis. *Trends in Parasitology* **38**: 642–659. https://doi.org/10.1016/j.pt.2022.05.007

Bojko J, Becnel J, Bessette E, *et al.* (2025). *Nosema* or *Vairimorpha*: Genomic/proteomic support to a complex socio-economic issue rooted in taxonomic change. *Journal of Invertebrate Pathology* **212**: 108376. https://doi.org/10.1016/j.jip.2025.108376

Bojko J, Ovcharenko M (2019). Pathogens and other symbionts of the *Amphipoda*: a review of their taxonomic diversity and pathological significance. *Diseases of Aquatic Organisms* **136**: 3–36. https://doi.org/10.3354/dao03321

Boratyn GM, Camacho C, Cooper PS, *et al.* (2013). BLAST: a more efficient report with usability improvements. *Nucleic Acids Research* **41**: W29–W33. https://doi.org/10.1093/nar/gkt282

Canning EU, Vávra J (2000). Phylum Microsporidia Balbiani, 1882. In '*Illus. Guid. to protozoa*,' 2nd edn. (JJ Lee, GF Leedale, P Bradbury, eds): 39–126. Allen Press: Lawrence.

Carstens BC, Pelletier TA, Reid NM, *et al.* (2013). How to fail at species delimitation. *Molecular Ecology* **22**: 4369–4383. https://doi.org/10.1111/mec.12413

Chen Y ping, Pettis JS, Zhao Y, *et al.* (2013). Genome sequencing and comparative genomics of honey bee microsporidia, *Nosema apis* reveal novel insights into host-parasite interactions. *BMC Genomics* **14**: 451. https://doi.org/10.1186/1471-2164-14-451

Chethana KWT, Manawasinghe IS, Hurdeal VG, *et al.* (2021). What are fungal species and how to delineate them? *Fungal Diversity* **109**: 1–25. https://doi.org/10.1007/s13225-021-00483-9

Darriba D, Taboada GL, Doallo R, *et al.* (2012). jModelTest 2: more models, new heuristics and parallel computing. *Nature Methods* **9**: 772–772. https://doi.org/10.1038/nmeth.2109

Eggers TH, Martens A (2001). A key to the freshwater *Amphipoda* (*Crustacea*) of Germany. *Lauterbornia* **42**: 1–68.

Flegel TW, Pasharawipas T (1995). A proposal for typical eukaryotic meiosis in microsporidians. *Canadian Journal of Microbiology* **41**: 1–11. https://doi.org/10.1139/m95-001

Franzen C (2008). Microsporidia: A Review of 150 Years of Research. *The Open Parasitology Journal* **2**: 1–34. https://doi.org/10.2174/1874421400802010001

Geneious development team (2025). Geneious Prime 2025.2.1. Available at https://www.geneious.com

Giari L, Fano EA, Castaldelli G, *et al.* (2020). The ecological importance of amphipod–parasite associations for aquatic ecosystems. *Water* **12**: 2429. https://doi.org/10.3390/w12092429

Grabner DS, Weigand AM, Leese F, *et al.* (2015). Invaders, natives and their enemies: distribution patterns of amphipods and their microsporidian parasites in the Ruhr Metropolis, Germany. *Parasites & Vectors* **8**: 419. https://doi.org/10.1186/s13071-015-1036-6

Hadziavdic K, Lekang K, Lanzen A, *et al.* (2014). Characterization of the 18S rRNA Gene for Designing Universal Eukaryote Specific Primers. (Voolstra CR, ed.) *PLoS ONE* **9**: e87624. https://doi.org/10.1371/journal.pone.0087624

Haine ER, Brondani E, Hume KD, *et al.* (2004). Coexistence of three microsporidia parasites in populations of the freshwater amphipod *Gammarus roeseli*: evidence for vertical transmission and positive effect on reproduction. *International Journal for Parasitology* **34**: 1137–1146. https://doi.org/10.1016/j.ijpara.2004.06.006

Harrison RG, Larson EL (2014). Hybridization, introgression, and the nature of species boundaries. *Journal of Heredity* **105**: 795–809. https://doi.org/10.1093/jhered/esu033

Huang W-F, Tsai S-J, Lo C-F, *et al.* (2004). The novel organization and complete sequence of the ribosomal RNA gene of *Nosema bombycis*. *Fungal Genetics and Biology* **41**: 473–481. https://doi.org/10.1016/j.fgb.2003.12.005

Ironside JE (2007). Multiple losses of sex within a single genus of *Microsporidia*. *BMC Evolutionary Biology* **7**: 48. https://doi.org/10.1186/1471-2148-7-48

Karaman GS, Pinkster S (1977). Freshwater *Gammarus* species from Europe, North Africa and adjacent regions of Asia (*Crustacea-Amphipoda*). Part I. *Gammarus pulex*-group and related species. *Bijdragen tot de Dierkunde* **47**: 1–97. https://doi.org/10.1163/26660644-04701001

Keeney DB, Waters JM, Poulin R (2007). Diversity of trematode genetic clones within amphipods and the timing of same-clone infections. *International Journal for Parasitology* **37**: 351–357. https://doi.org/10.1016/j.ijpara.2006.11.004

Kelly A, Dunn AM, Hatcher MJ (2002). Incomplete feminisation by the microsporidian sex ratio distorter, *Nosema granulosis*, and reduced transmission and feminisation efficiency at low temperatures. *International Journal for Parasitology* **32**: 825–831. https://doi.org/10.1016/S0020-7519(02)00019-X

Krebes L, Zeidler L, Frankowski J, *et al.* (2014). (Cryptic) sex in the microsporidian *Nosema granulosis* – Evidence from parasite rDNA and host mitochondrial DNA. *Infection, Genetics and Evolution* **21**: 259–268. https://doi.org/10.1016/j.meegid.2013.11.007

Królikowska K, Zawal A, Grabowski M, *et al.* (2024). First DNA barcode reference library for water mites of the ancient Lake Ohrid reveals high diversity and lineage endemism. *Journal of Great Lakes Research* **50**: 102344. https://doi.org/10.1016/j.jglr.2024.102344

Leiro J, Ortega M, Iglesias R, *et al.* (1996). *Pleistophora finisterrensis* n. sp., a microsporidian parasite of blue whiting *Micromesistius poutassou*. *Systematic Parasitology* **34**: 163–170. https://doi.org/10.1007/BF00009384

Nadler SA, De León GP-P (2011). Integrating molecular and morphological approaches for characterizing parasite cryptic species: implications for parasitology. *Parasitology* **138**: 1688–1709. https://doi.org/10.1017/S003118201000168X

Naegeli K (1857). Über die neue Krankheit der Seidenraupe und verwandte Organismen. *Botanische Zeitung* **15**: 760–761.

Ovcharenko MO, Bacela K, Wilkinson T, *et al.* (2010). Cucumispora dikerogammari n. gen. (Fungi: Microsporidia) infecting the invasive amphipod *Dikerogammarus villosus*: a potential emerging disease in European rivers. *Parasitology* **137**: 191–204. https://doi.org/10.1017/S0031182009991119

Paramá A, Arranz JA, Álvarez MF, *et al.* (2006). Ultrastructure and phylogeny of *Philasterides dicentrarchi* (*Ciliophora, Scuticociliatia*) from farmed turbot in NW Spain. *Parasitology* **132**: 555–564. https://doi.org/10.1017/S0031182005009534

Park E, Poulin R (2021). Revisiting the phylogeny of microsporidia. *International Journal for Parasitology* **51**: 855–864. https://doi.org/10.1016/j.ijpara.2021.02.005

Pieniazek NJ, da Silva AJ, Slemenda SB, *et al.* (1996). *Nosema trichoplusiae* is a synonym of *Nosema bombycis* based on the sequence of the small subunit ribosomal RNA coding region. *Journal of Invertebrate Pathology* **67**: 316–317. https://doi.org/10.1006/jipa.1996.0049

Puillandre N, Brouillet S, Achaz G (2021). ASAP: assemble species by automatic partitioning. *Molecular Ecology Resources* **21**: 609–620. https://doi.org/10.1111/1755-0998.13281

Quiles A, Bacela-Spychalska K, Teixeira M, *et al.* (2019). Microsporidian infections in the species complex *Gammarus roeselii* (*Amphipoda*) over its geographical range: Evidence for both host-parasite co-diversification and recent host

shifts. *Parasites and Vectors* **12**: 327. https://doi.org/10.1186/s13071-019-3571-z

Quiles A, Wattier RARA, Bacela-Spychalska K, *et al.* (2020). *Dictyocoela* microsporidia diversity and co-diversification with their host, a gammarid species complex (*Crustacea, Amphipoda*) with an old history of divergence and high endemic diversity. *BMC Evolutionary Biology* **20**: 1–17. https://doi.org/10.1186/s12862-020-01719-z

Quiles A, Rigaud T, Wattier RA, *et al.* (2021). Wide geographic distribution of overlooked parasites: Rare microsporidia in *Gammarus balcanicus*, a species complex with a high rate of endemism. *International Journal for Parasitology: Parasites and Wildlife* **14**: 121–129. https://doi.org/10.1016/j.ijppaw.2021.01.004

Ronquist F, Huelsenbeck JP (2003). MrBayes 3: Bayesian phylogenetic inference under mixed models. *Bioinformatics* **19**: 1572–1574. https://doi.org/10.1093/bioinformatics/btg180

Sarabeev V, Balbuena JA, Jarosiewicz A, *et al.* (2023a). Disentangling the determinants of symbiotic species richness in native and invasive gammarids (*Crustacea, Amphipoda*) of the Baltic region. *International Journal for Parasitology* **53**: 305–316. https://doi.org/10.1016/j.ijpara.2023.02.006

Sarabeev V, Ovcharenko M, Jarosiewicz A, *et al.* (2023b). Database on eukaryotic symbionts of native and invasive gammarids (*Crustacea, Amphipoda*) in the Baltic region of Poland with information on water parameters for sampling sites. *Data in Brief* **49**: 109308. https://doi.org/10.1016/j.dib.2023.109308

Sarabeev V, Balbuena JA, Oros M, *et al.* (2024). Symbiotic species diversity can explain invasion success and host–parasite system stability: The case of gammarid hosts. *Ecosphere* **15**: e4946. https://doi.org/10.1002/ecs2.4946

Sarabeev V, Rashydov A, Lisitsyna O, *et al.* (2025). A new family for *Cephalotrema elasticum* (Digenea) based on molecular data, with notes on the status of the definitive host population. *Scientific Reports* **15**: 33771. https://doi.org/10.1038/s41598-025-98898-w

Sarabeev V, Ovcharenko M (2024). Eukaryotic symbionts of native and non-native gammarids (*Crustacea: Amphipoda: Gammaroidea*) inhabiting Pomeranian coastal waters of Poland. In 'Biotyczne i abiotyczne zasoby Pomorza Środkowego. T. II.': 195–213. Wydawnictwo Naukowe Uniwersytetu Pomorskiego w Slupsku.

Scholz T (2024). Gaps in parasitological research in the molecular era. *Trends in Parasitology* **40**: 283–291. https://doi.org/10.1016/j.pt.2024.02.005

Shaw JC, Henriksen EH, Knudsen R, *et al.* (2020). High parasite diversity in the amphipod Gammarus lacustris in a subarctic lake. *Ecology and Evolution* **10**: 12385–12394. https://doi.org/10.1002/ece3.6869

Sievers F, Wilm A, Dineen D, *et al.* (2011). Fast, scalable generation of high-quality protein multiple sequence alignments using Clustal Omega. *Molecular Systems Biology* **7**:. https://doi.org/10.1038/msb.2011.75

Sokolova YY, Fuxa JR (2008). Biology and life-cycle of the microsporidium *Kneallhazia solenopsae* Knell Allan Hazard 1977 gen. n., comb. n., from the fire ant *Solenopsis invicta*. *Parasitology* **135**: 903–929. https://doi.org/10.1017/S003118200800440X

Sokolova YY, Overstreet RM (2018). A new microsporidium, *Apotaspora heleios* n. g., n. sp., from the Riverine grass shrimp *Palaemonetes paludosus* (*Decapoda: Caridea: Palaemonidae*). *Journal of Invertebrate Pathology* **157**: 125–135. https://doi.org/10.1016/j.jip.2018.05.007

Sprague V, Becnel JJ, Hazard EI (1992). Taxonomy of phylum *Microspora*. *Critical Reviews in Microbiology* **18**: 285–395. https://doi.org/10.3109/10408419209113519

Stentiford GD, Bateman KS, Feist SW, *et al.* (2013a). Plastic parasites: Extreme dimorphism creates a taxonomic conundrum in the phylum *Microsporidia*. *International Journal for Parasitology* **43**: 339–352. https://doi.org/10.1016/j.ijpara.2012.11.010

Stentiford GD, Feist SW, Stone DM, *et al.* (2013b). Microsporidia: diverse, dynamic, and emergent pathogens in aquatic systems. *Trends in Parasitology* **29**: 567–578. https://doi.org/10.1016/j.pt.2013.08.005

Stentiford GD, Ross S, Minardi D, *et al.* (2018). Evidence for trophic transfer of *Inodosporus octospora* and *Ovipleistophora arlo* n. sp. (*Microsporidia*) between crustacean and fish hosts. *Parasitology* **145**: 1105–1117. https://doi.org/10.1017/S0031182017002256

Stentiford GD, Dunn AM (2014). *Microsporidia* in Aquatic Invertebrates. In '*Microsporidia*.': 579–604. (Wiley)

Stratton CE, Bolds SA, Reisinger LS, *et al.* (2024). *Microsporidia* and invertebrate hosts: genome-informed taxonomy surrounding a new lineage of crayfish-infecting *Nosema* spp. (*Nosematida*). *Fungal Diversity* **128**: 167–190. https://doi.org/10.1007/s13225-024-00543-w

Tedersoo L, Sánchez-Ramírez S, Kõljalg U, *et al.* (2018). High-level classification of the *Fungi* and a tool for evolutionary ecological analyses. *Fungal Diversity* **90**: 135–159. https://doi.org/10.1007/s13225-018-0401-0

Terry RS, Smith JE, Bouchon D, *et al.* (1999). Ultrastructural characterisation and molecular taxonomic identification of *Nosema granulosis* n. sp., a transovarially transmitted feminising (TTF) microsporidium. *The Journal of Eukaryotic Microbiology* **46**: 492–499. https://doi.org/10.1111/j.1550-7408.1999.tb06066.x

Terry RS, Macneil C, Dick JTA, *et al.* (2003). Resolution of a taxonomic conundrum: an ultrastructural and molecular description of the life cycle of *Pleistophora mulleri* (Pfeiffer 1895; Georgevitch 1929). *Journal of Eukaryotic Microbiology* **50**: 266–273. https://doi.org/10.1111/j.1550-7408.2003.tb00133.x

Tokarev YS, Huang W-F, Solter LF, *et al.* (2020). A formal redefinition of the genera *Nosema* and *Vairimorpha* (*Microsporidia: Nosematidae*) and reassignment of species based on molecular phylogenetics. *Journal of Invertebrate Pathology* **169**: 107279. https://doi.org/10.1016/j.jip.2019.107279

Tosun O (2020). A new isolate of *Nosema fumiferanae* (*Microsporidia: Nosematidae*) from the date moth *Apomyelois (Ectomyelois) ceratoniae* , Zeller, 1839 (*Lepidoptera: Pyralidae*). *Parasitology* **147**: 1461–1468. https://doi.org/10.1017/S0031182020001481

Trzebny A, Slodkowicz-Kowalska A, Becnel JJ, *et al.* (2020). A new method of metabarcoding Microsporidia and their hosts reveals high levels of microsporidian infections in mosquitoes (*Culicidae*). *Molecular Ecology Resources* **20**: 1486–1504. https://doi.org/10.1111/1755-0998.13205

Weigand AM, Kremers J, Grabner DS (2016). Shared microsporidian profiles between an obligate (*Niphargus*) and facultative subterranean amphipod population (*Gammarus*) at sympatry provide indications for underground transmission pathways. *Limnologica* **58**: 7–10. https://doi.org/10.1016/j.limno.2016.01.005

Wijayawardene N, Hyde KD, Al-Ani LKT, *et al.* (2020). Outline of *Fungi* and fungus-like taxa. *Mycosphere* **11**: 1060–1456. https://doi.org/10.5943/mycosphere/11/1/8

Willis AR, Reinke AW (2022). Factors that determine *Microsporidia* infection and host specificity. In '*Microsporidia*. Exp. Suppl. vol 114.': 91–114

Xiong X, Geden CJ, Tan Y, *et al.* (2024). Genome structure, evolution, and host shift of *Nosema*. *Biology* **13**: 952. https://doi.org/10.3390/biology13110952

Zhu X, Wittner M, Tanowitz HB, *et al.* (1993). Small subunit rRNA sequence of *Enterocytozoon bieneusi* and its potential diagnostic role with use of the polymerase chain reaction. *Journal of Infectious Diseases* **168**: 1570–1575. https://doi.org/10.1093/infdis/168.6.1570

Supplementary Material: http://fuse-journal.org/

File 1. Morphologic description of hapantotypes of Nosema slupiense sp. nov. with diagnostic comparison of microsporidia parasitising Gammarus pulex.

Table S1. Alignment of partial sequences (992 bp) of 18S rDNA gene for 42 sequences of Nosema spp. used in the phylogenetic analysis.

Table S2. Alignment of partial sequences of Nosema spp. (871 bp, F2 and F4 fragments of RPB1 gene) for 42 sequences used in phylogenetic analysis, including Vairimorpha species as outgroup.

Fig. S1. Sequence alignment of *Nosema* spp. for both F2 and F4 fragments of the *RPB1* marker, illustrating SNP positions. The highlighted characters [#863 (state A), #884 (A), #905 (A), and #1,166 (C)] represent pure single-character attributes; in other words, these are unambiguous synapomorphies that uniquely characterize and diagnose *Nosema slupiense sp. nov.* The primer sets F2F-F2R and F4F-F4R are mapped on the consensus sequence. Shaded "N" indicates the absence of nucleotides. The sequence labels are as in Fig. 1.

Fig. S2. Dissimilarity heatmap (bp number\%) of *Nosema* spp. based on 992 bp of the 18S rDNA. Sequences obtained in the present study are in bold with the number of duplicates in parentheses. The sequence labels are as in Fig. 1.

Fig. S3. Dissimilarity heatmap (bp number\%) of *Nosema* spp. based on 871 bp of F2 and F4 fragments of the *RPB1*. Sequences obtained in the present study are in bold with the number of duplicates in parentheses. The sequence labels are as in Fig. 1.

Fig. S4. Sequence alignment of host isolates (KSGP15, KSGP20, KSGP23, KSGP29, KSGP45, KSGP46, KSGP47, KSGP53) for the COI-5P fragment of the mitochondrial genome infected with the *Nosema* spp. studied herein and sequences of *Gammarus pulex* BIN BOLD:ACH6832.